

Revisions and responses to reviewers' comments

First of all, we would like to thank the reviewers for their comments and suggestions which significantly improve the presentations and interpretations in our revised manuscript. Based on the reviewers' comments, we have made major revisions to the manuscript. The reviewers' original comments are shown in italics and our responses are given in normal fonts.

Response to Anonymous Referee #1

This study demonstrates an increasing trend in SO₂ over the northwestern region in China, in contrast to a well-established decreasing trend already reported for Eastern China. Shen et al., 2016 presented similar results before, however, here, the authors perform regression analysis/MK test, and 'a source detection approach to derive source strengths' using OMI-derived SO₂ column density. They also report ~ 30-50% contribution of SO₂ emissions over the two northwestern regions from two energy industrial parks. This work can be accepted for publication upon addressing the following suggestions.

1. A more rigorous and thorough analysis is required to confirm that the OMI-retrieved SO₂ column densities can be used to derive/estimate the increasing trend in SO₂ emissions/concentrations over these regions. Here, authors use Level-3 SO₂ data at a particular spatial resolution with a constant AMF of 0.35. I would suggest a more detailed and in-depth study using the satellite SO₂ column density dataset; in terms of AMFs, spatial resolutions, various data filtering methods, sampling, averaging etc. and its impact on the results demonstrated here. This sort of a scientific analysis is required in order to come within the scope of ACP (rather than describing the trend analysis and spatiotemporal pattern of SO₂ sources). McLinden et al., Fioletov et al., and Krotkov et al. papers are good references for this. Also, two years of in situ data over 188 sites offer a valuable piece of information (for example, L134:138: representativeness issues should have been addressed/described more carefully) to further test/evaluate satellite data (in addition to the supplementary figure and table). Also, describe in detail how the uncertainties in various datasets impact the results.

Response:

As we stated in our paper (line 119-122), we used Level-3 SO₂ data at a particular spatial resolution with a constant AMF of 0.36 but the SO₂ column density was adjusted by AMF values in China. Following the Reviewer's suggestions, we have rephrased text regarding the satellite data applied in the present study. In revised section 2.1, we introduced more detailed descriptions of the source, spatial resolutions, and potential errors of satellite data (line 86-122). In new sections 2.4 and

2.5, we added more details in the source detection algorithm developed by McLinden et al. and Fioletov et al. The sources of errors in determining the overall uncertainty of the SO₂ emission estimation as well as their impact on the results were discussed (line 219-230). We further added the comments on the causes of the inconsistency between SO₂ VCD and monitored data (line 257-278 of the revised manuscript).

We have quantified the uncertainties in the SO₂ emissions derived from OMI measurements in the two major point sources in northwestern China by running the source detection model repeatedly for 10,000 times using Monte Carlo method. Results show the standard deviation of -35 to 122 kt/yr for SO₂ emissions in NECIB and -29 to 95 kt/yr for SO₂ emissions in MEIB from 2005 to 2015 which are presented in Fig. 11a and b, respectively (line 219-230 of the revised manuscript)

2. Need to correct for grammatical mistakes throughout the paper (examples; L2: economic growth; L9: reduction of; L127: but the both; L133: such the inconsistency; L200: an significant; 412: desert and Gopi? : : :). Also, loose/empty sentences, and repetitions should be corrected while revising the paper. Change 'SO₂' to 'SO₂' for all the figures.

Response:

We have made every effort to improve language and taken more careful proofreading of the revised manuscript. Those spells and language errors have been corrected (e.g. 'destert and gobi' changed to Gobi desert) . We have changed 'SO2' to 'SO₂' in all the figures.

3. L81:82: try avoiding the point no.2, you can mention that, however, it's already an established point?

Response:

We thank the Reviewer for his/her suggestion. We have rewritten the second objective of this paper as "identify main causes contributing to the enhanced SO₂ emission in northwestern China" (line 81-82 of the revised manuscript).

4. Section 2.1: describe more details of satellite SO₂ data, error sources etc. This is the most important part of this paper.

Response:

As our above response to the Reviewer's comment, following the Reviewer's suggestions, we have rewritten the description of satellite data (section 2.1). We also added the source, spatial resolutions, error, and uncertainties of satellite data used in China in this study in two new sections 2.4 and 2.5.

5. L101:118: *Better if you describe figures and tables in the results section. Describe just the 'materials and methods' in this section.*

Response:

Following the Reviewer's suggestion, we have rearranged the structure of Data and Methods section. We added the new section 2.5 (satellite data validation), and moved the discussions on the results presented in Table S2, Figure S1. Figures 2 and 3 were presently presented in Supplement but moved to Data and Methods section following the suggestion from a reviewer.

6. L133:134 *skeptical of in situ? So, first, describe the dataset, and associated errors, and then describe your figures/results in that context.*

Response:

Following the Reviewer's comments and suggestions, in the revised manuscript, we have analyzed the causes leading to the inconsistency between SO₂ VCD and monitored data (line 257-278 of the revised manuscript).

7. *Column density and emissions are correlated (supplementary figure and table). However, describe briefly why there are not linearly related; also, cite some relevant papers relating column density to emissions and surface concentrations (for example, using atmospheric models).*

Response:

We thank the Reviewer for his/her suggestion. We have conducted new analysis on the inconsistency between SO₂ emission and satellite observations data (line 283-298 of the revised manuscript).

8. L134:139: *how about using higher resolutions to address the issues of representativeness? Also, these are loose/empty sentences.*

Response:

We agree that higher resolutions can reduce errors between SO₂ VCD and monitored data. However, given the unavailability of data, only annual average monitored SO₂ concentration in Urumqi city can be collected from the official data, which is spatially averaged concentration over several monitoring sites across the city. This disagreement is unlikely resulted from the spatial resolution of satellite and measured SO₂ data because good agreements between SO₂ VCD and monitored concentrations can be seen in other cities. As aforementioned, we have discussed the causes resulting

in the inconsistency between SO₂ VCD and monitored data in the revised manuscript (line 257-278).

9. L150:153: Those publications report some uncertainty estimates; report them here; and describe your figure in that context; more carefully.

Response:

Following the Reviewer's suggestions. We have added the uncertainties of SO₂ emission in China, and described Figure 3 (line 293-303 of the revised manuscript).

10. L153:156: revise/avoid this sentence.

Response:

This sentence has been rephrased in the revised paper (line 303-306).

11. L157:162: briefly mention the socioeconomic data? GDP? why per capita emissions used?

Response:

We have added the detail socioeconomic data in the revised manuscript (line 142-144). In general, higher SO₂ emissions are reported in those populated and industrialized regions. The use of per capita emission was to highlight the significance of SO₂ emission in northwestern China and the fairness in accounting for SO₂ emissions across China.

12. Results and discussion section is disorganized throughout. For the results section, first describe the decreases in SO₂ over eastern China (as already reported in earlier publications), and focus more on the northwestern region (regions with increasing trend; this is the novel aspect of this paper?) in a separate sub-section.

Response:

Following the Reviewer's suggestion, we have reorganized Results and Discussion section. In subsection 3.1 'OMI measured SO₂ in China', we briefly discussed spatial-temporal distribution and fluctuations of SO₂ VCD in China with focus on eastern and southern China. In subsection 3.2 'OMI measured SO₂ 'hot spots' in northwestern China', we highlighted two SO₂ contaminated 'hot spots' featured by increasing SO₂ VCDs in two large-scale energy industrial bases. In subsection 3.3 'OMI SO₂ time series and step change point year in northwestern China', we extended our discussions and analysis from the increasing SO₂ VCD in the two 'hot spots' to entire northwestern China which might be linked with SO₂ emissions in those energy

industrial bases. To be consistency with the new paper flow in the section, we moved Fig. 8 to subsection 3.1 as Fig. 6.

13. Figure 4: color bar should have the units.

Response:

Done!

14. L385:393: describe 'source detection approach' (describe vertical column vs 'burden'; 'emission burden' a rate?) in the method section more clearly; and describe Figure 10/11 here in the results section itself. Better to overlay the column density data in figure 11. Also, a map of column density possible in figure 10 to see it in the context of these burden maps?

Response:

Detailed source detection approach has been added to Date and Method section in the revised paper. We also presented detailed descriptions of SO₂ emission estimate in new section 2.4. There was an error in previous Fig. 10. In figure caption and corresponding discussions we talked about SO₂ emission burden. In the revised paper Fig. 10 shows SO₂ VCD. Corresponding discussions were also revised (line 487-494). The estimated SO₂ emissions using the source detection algorithm (Fioletove et al. 2015, 2016), VCDs, and their respective fractions are illustrated in revised Fig. 11.

15. L462: mention about Particulate Matter (PM) in the introduction section itself.

Response:

We have deleted this phrase.

Response to Anonymous Referee #2

The manuscript discusses SO₂ changes observed by OMI and links them to the national regulations of SO₂ emissions. The paper demonstrates again the usefulness of satellite monitoring of air pollutions in China, the world largest SO₂ emitter. It is shown that major changes in OMI records are linked to the emission reduction legislation. In general, the paper is well written, although some places require clarification. It can be published after minor revisions.

1. It is difficult to follow geographical names used by the authors. For example, Midong appears on p. 8, l. 145, without any mentioning of its location. As I understand, it is a district, but then the authors are talking about Urumqi-Midong region (p. 12, l. 241) and Midong industrial park. Give more information about the cities and regions, provide cities coordinates, show all cities from Figure 2 in Figure 1.

Response:

We have revised Figure 1. We also added the selected cities shown in Fig. 2 to Figure 1, and marked several "hot spots" regions, including Urumqi-Midong region and Energy Golden Triangle (EGT), Ningdong energy chemical industrial base (NECIB), and Midong energy industrial base (MEIB), in northwestern China in Figure 1.

2. P.7, l. 117, Figure 2. There is an explanation why the Urumqi plot is different from the others. Note that the measured SO₂ concentration at Urumqi is the highest among all cities shown in Figure 2, while the OMI VCD values are the lowest. It suggests that the monitoring stations are located very close to the emission source (a power plant south of Urumqi?) and the emissions are not very large. The SO₂ VCD values of about 0.1 DU are close to the noise level. The emission source is probably not large enough to produce elevated SO₂ values in OMI data.

Response:

The measured SO₂ concentration in Urumqi is the highest among all cities as shown in Fig. 2. However, as the Reviewer noted, the OMI SO₂ VCD value in Urumqi was lower than other selected cities. This may be due to the error from systematic biases in OMI-retrieved SO₂ VCD. Here we used the level 3 OMI PBL SO₂ VCD data produced by the PCA retrievals to estimate the spatiotemporal variation in SO₂ pollution in China. The PCA retrievals have a negative bias over some highly reflective surfaces such as many places in the Sahara (up to -0.5 DU in monthly mean). The systematic bias of PCA retrieval is estimated at ~-0.5 DU for regions between 30°S and 30°N and ~-0.7-0.9 DU in relatively high latitude regions. Located in northwestern China and covered by Gobi desert in the surrounding regions of Urumqi, lower SO₂ VCD might be yielded by the PCA retrieval over Urumqi

compared with other cities (line 264-278). This point has been added to the revised paper.

3. P.8, l. 145, Figure 2. SO₂ emissions shown in Figure 2 for Midong are under 25 kt per year. OMI is not sensitive enough to see such emission sources, its sensitivity level is 30-40 kt per year (Fioletov et al., 2016). If there is a OMI hotspot in the area, that it is likely that the emissions from the source responsible for that hotspot are not in the emission inventory.

Response:

We agree with the Reviewer's comments. As shown in Figure 3, the OMI measured SO₂ VCD in Urumqi-Midong from 2008 to 2012 was approximately 0.2 DU that was comparable with that in the EGT. However, SO₂ emission in Urumqi-Midong was only 4% of that in the EGT in 2012. In particular, SO₂ emission in Urumqi-Midong was 0.5% of that in the EGT from 2008 to 2010. This is probably because SO₂ emission sources were not reported in emission inventory. Atmospheric removal and advection processes may also contribute to the inconsistency between monitored and satellite observations. These arguments have been added to the revised manuscript (line 287-303).

4. P. 19, l. 388-393 and Figure 10. This part is not clear. Papers McLinden et al., 2016, and Fioletov et al., 2016, used OMI Level 2 data merged with the wind profiles to estimate emissions from point sources. As I understand, the authors used Level 3 gridded data. What wind data were used and how the time was determined for grid cells? What is actually shown in Figure 10? The legend is in molecules, i.e., it can be interpreted as total SO₂ mass. The caption says that it is in DU. Or, is it the emission rate? If the authors estimated emissions, they should elaborate more on the results. Do the estimated emissions agree with the reported ones? Are there any other sources within the areas shows in the two squares of Figure 10? If so, why are they not on the plot?

Response:

We thank the Reviewer to point out this confusion. There was an error in previous Fig. 10. In old figure 10 caption and corresponding discussions we talked about SO₂ emission burden. In the revised paper Fig. 10 shows SO₂ VCD. Corresponding discussions were also revised (line 487-494). The estimated SO₂ emissions using the source detection algorithm (Fioletove et al. 2015, 2016), VCDs, and their respective fractions are illustrated in revised Fig. 11. In a new subsection 2.4, we presented the details of SO₂ emission estimate using the source detection algorithm developed by Fioletov et al. (2015, 2016) in which wind speed data were used.

We estimated the SO₂ burden (in number of molecules in 10²⁶) which represents the total SO₂ mass. Again we thank the reviewer to indicate the error in the unit of SO₂ burden. Now the revised Fig. 10 shows SO₂ VCD with the unit of DU. Revised Fig. 11 shows the estimated SO₂ emission with the unit of kt/yr (Fig. 11a and b) and VCD with the unit of DU (Fig. 11c and d) in MEIB and NECIB, respectively.

5. P.19, l. 393 and p. 20, 398, also Figure 11. The authors are talking about “SO₂ burthen” and then “SO₂ emission burdens” both in molecules. Are these two terms the same? If they are in molecules, they represent the total mass integrated over an area and it is more convenient to show them in tones. If they represent emissions, they should be in units of mass per unit of time. Something is missing here.

Response:

Please see our last response to the Reviewer. Revised Fig. 11 now illustrates the estimated SO₂ emission (Fig. 11a and b) and VCD (Fig. 11c and d) in MEIB and NECIB using the source detection algorithm. In text, "SO₂ emission burdens" have been changed to "SO₂ emission".

6. P. 35, Table 1. What are the units in the OMI SO₂ VCD column? Are the values in % per year for all columns except the last two where the values are in % per 5 years? Please clarify.

Response:

Table 1 presents the annual growth rate for OMI SO₂ VCD and economic activities for individual provinces and municipality during 2005-2014 (% yr⁻¹). For OMI SO₂ VCD column, they represented annual growth rate of spatially averaged SO₂ VCD in the individual regions. In Table 1, the last two columns represented SO₂ emission reduction plan during the 11th and 12th Five-Year Plan period, released by Chinese government every five years.

OMI measured increasing SO₂ emissions due to energy industry expansion and relocation in Northwestern China

Authors:

Zaili Ling¹, Tao Huang^{1,*}, Yuan Zhao¹, Jixiang Li¹, Xiaodong Zhang¹, Jinxiang Wang¹, Lulu Lian¹, Xiaoxuan Mao¹, Hong Gao¹, Jianmin Ma^{2,1,3,*}, ~~Ma^{1,2,3,*}~~

Affiliations:

¹Key Laboratory for Environmental Pollution Prediction and Control, Gansu Province, College of Earth and Environmental Sciences, Lanzhou University, Lanzhou 730000, P. R. China

²Laboratory for Earth Surface Processes, College of Urban and Environmental Sciences, Peking University, Beijing, 100871, China

³CAS Center for Excellence in Tibetan Plateau Earth Sciences, Chinese Academy of Sciences, Beijing, 100101, China

Corresponding author: Jianmin Ma, Tao Huang

College of Earth and Environmental Sciences, Lanzhou University, 222, Tianshui South Road, Lanzhou 730000, China

Email: jianminma@lzu.edu.cn; huangt@lzu.edu.cn

1 Abstract

2 The rapid growth of economy ~~growth~~ makes China the largest energy consumer and
3 ~~sulfur~~sulphur dioxide (SO₂) emitter in the world. In this study, we estimated the trends
4 and step changes in the planetary boundary layer (PBL) vertical column density (VCD)
5 of SO₂ from 2005 to 2015 over China measured by the Ozone Monitoring Instrument
6 (OMI). We show that these trends and step change years coincide with the effective
7 date and period of the national strategy for energy development and relocation in
8 northwestern China and the regulations in the reduction of SO₂ emissions. Under the
9 national regulations in the ~~reduction~~ SO₂ emissions reduction in eastern and southern
10 China, SO₂ VCD in the Pearl River Delta (PRD) of southern China exhibited the
11 largest decline during 2005-2015 at a rate of $-7\% \text{ yr}^{-1}$, followed by the North China
12 Plain (NCP) ($-6.7\% \text{ yr}^{-1}$), Sichuan Basin ($-6.3\% \text{ yr}^{-1}$), and Yangtze River Delta (YRD)
13 ($-6\% \text{ yr}^{-1}$), respectively. The Mann-Kendall (MK) test reveals the step change points
14 of declining SO₂ VCD in 2009 for the PRD and 2012-2013 for eastern China
15 responding to the implementation of SO₂ control regulation in these regions. In
16 contrast, the MK test and regression analysis also revealed increasing trends of SO₂
17 VCD in northwestern China, particularly for several "hot spots" featured by growing
18 SO₂ VCD in those large-scale energy industry bases~~spots~~ in northwestern China. The
19 enhanced SO₂ VCD is potentially attributable to increasing SO₂ emissions due to the
20 development of large-scale energy industry bases in energy-abundant northwestern
21 China under the national strategy for the energy safety of China in the 21st century.
22 We show that these large-scale energy industry bases could overwhelm the trends and

23 changes in provincial total SO₂ emissions in northwestern China and contributed
24 increasingly to the national total SO₂ emission in China. Given that northwestern
25 China is more ecologically fragile and uniquely susceptible to atmospheric pollution
26 as compared with the rest of China, increasing SO₂ emissions in this part of China
27 should not be overlooked and merit scientific research.

28

29 **1. Introduction**

30 Sulfur dioxide (SO₂) is one of the criteria air pollutants emitted from both
31 anthropogenic and natural sources. The combustions of sulfur-containing fuels, such
32 as coal and oil, are the primary anthropogenic emitters, which contributed to the half
33 of total SO₂ emissions (Smith et al., 2011; Lu et al., 2010; Stevenson et al., 2003;
34 Whelpdale et al., 1996). With the rapid economic growth in the past decades, China
35 has become the world's largest energy consumer accounting for 23% of global energy
36 consumption in 2015 (BIEE, 2016). Coal has been a dominating energy source in
37 China and accounted for 70% of total energy consumption in 2010 (Kanada et al.,
38 2013). The huge demand ~~forte~~ coal and its high sulfur content make China the largest
39 SO₂ emission source in the world (Krotkov et al., 2016; Su et al., 2011), which also
40 accounted for two-third of Asia's total SO₂ emission (Ohara et al., 2007). From 2000
41 to 2006, the total SO₂ emission in China increased by 53% at an annual growth rate of
42 7.3% (Lu et al., 2010). To reduce SO₂ emission, from 2005 onward the Chinese
43 government has issued and implemented a series of regulations, strategies, and SO₂
44 control measures, leading to a drastic decrease of SO₂ emission, particularly in eastern

45 and southern China (Lu et al., 2011; Li et al., 2010).

46 Recently, two research groups led by NASA (National Aeronautics and Space
47 Administration) and Lanzhou University of China published almost simultaneously
48 the temporal and spatial trends of SO₂ in China from 2005 to 2015 using the OMI
49 retrieved SO₂ PBL column density after the OMI is ~~launched~~^{launched} for 11 years
50 (Krotkov et al., 2016; Shen et al., 2016). The results reported by the two groups
51 revealed ~~the~~ widespread decline of SO₂ in eastern China for the past decade. Shen et al.
52 noticed, however, that, in contrast to dramatic decreasing SO₂ emissions in densely
53 populated and industrialized eastern and southern China, the OMI measured SO₂ in
54 northwestern China appeared not showing a decreasing trend. This is likely resulted
55 from the energy industry relocation and development in energy-abundant
56 northwestern China in the past decades under the national strategy for China's energy
57 development and safety during the 21st century. Concern is raised ~~about~~^{for} the
58 potential impact of SO₂ emissions on the ecological environment and health risk in
59 northwestern China because high SO₂ emissions could otherwise damage the rigorous
60 ecological environment in this part of China, featured by very low precipitation and
61 sparse vegetation coverage which reduce considerably the atmospheric removal of air
62 pollutants (Ma and Xu, 2017).

63 To assess and evaluate the risks of the ecological environment and public to the
64 growing SO₂ emissions in northwestern China, it is necessary to investigate the
65 spatiotemporal distributions of SO₂ concentrations and emissions. However, the
66 ground measurements of ambient SO₂ are scarce temporally and spatially in China,

67 and often subject to ~~significant~~large errors and uncertainties. Owing to the rapid
68 progresses in the remote sensing techniques, satellite retrieval of air pollutants has
69 become a powerful tool ~~for~~in the assessment of emissions and spatiotemporal
70 distributions of air pollutants. In recent several years, OMI (Dutch Space, Leiden, The
71 Netherlands, embedded on Aura satellite) retrieved SO₂ column concentrations have
72 been increasingly applied to elucidate the spatiotemporal variation of global and
73 regional SO₂ levels and its emissions from large point sources, and evaluate the
74 effectiveness of SO₂ control policies and measures (Krotkov et al., 2016; McLinden et
75 al., 2015, 2016; Ialongo et al., 2015; Fioletov et al., 2015, 2016; Wang et al., 2015;
76 Li et al., 2010). The decadal operation of the OMI provides the relatively long-term
77 SO₂ time series data with a high spatial resolution which are particularly useful for
78 assessing the changes and trends in SO₂ emissions induced by national regulations
79 and strategies. The present study aims to (1) ~~determine~~assess the spatiotemporal
80 variations of SO₂ and its trend under the national ~~plan~~strategy for energy industry
81 development in northwestern China by making use of the OMI-measured SO₂ data
82 during 2005-2015; (2) to identify leading causes contributing to the enhanced SO₂
83 emission in northwestern China.~~further examine the usefulness of the satellite remote~~
84 ~~sensing of air quality.~~

85

86 **2 Data and methods**

87 **2.1 Satellite data**

88 The OMI Ozone Monitoring Instrument (OMI) was launched on July 15, 2004,

89 on the EOS Aura satellite, which is in a sun-synchronous ascending polar orbit with
90 1:45 pm local equator crossing time. It is an ultraviolet/visible (UV/VIS) nadir solar
91 backscatter spectrometer, which provides nearly global coverage in one day, with a
92 spatial resolution of 13 km×24 km (Levelt et al. 2006a, 2006b). It provides global
93 measurements of ozone (O₃), SO₂, NO₂, HCHO and other pollutants on a daily basis.
94 The OMI uses spectral measurements between 310.5 and 340 nm in the UV-2 to
95 detect anthropogenic SO₂ pollution in the lowest part of the atmosphere (Li et al.,
96 2013). The instrument is sensitive enough to detect the near-surface SO₂. Previously,
97 the OMI PBL SO₂ data were produced using the Band Residual Difference (BRD)
98 algorithm (Krotkov et al., 2006), which have large noise and unphysical biases
99 particularly at high latitudes (Krotkov et al., 2008). Subsequently, a principal
100 component analysis (PCA) algorithm was applied to retrieve SO₂ column densities.
101 This approach greatly reduces biases and decreases the noise by a factor of 2,
102 providing greater sensitivity to anthropogenic emissions (Li et al., 2013).

103 In the present study, we—We collected the level 3 OMI daily planetary
104 boundary layer (PBL) SO₂ vertical column density (VCD) data in Dobson units (1
105 DU=2.69×10¹⁶ molecules cm⁻²) produced by the ~~principal component analysis (PCA)~~
106 algorithm (Li et al., 2013). The spatial resolution is 0.25°×0.25° latitude/ longitude,
107 available at Goddard Earth Sciences Data and Information Services Center
108 (http://disc.sci.gsfc.nasa.gov/Aura/data-holdings/OMI/omso2_v003.shtml). The systematic
109 bias of PCA retrievals is estimated as ~0.5 DU for regions between 30°S and 30°N. The
110 bias increases to ~0.7-0.9 DU for high latitude areas with large slant column O₃ but is still a

111 ~~factor of two smaller than that from BRD retrievals~~
112 ~~(<https://disc.gsfc.nasa.gov/Aura/data-holdings/OMI/documents/v003/omso2readme-v120-2>~~
113 ~~0140926.pdf). As a result, the PCA~~~~This algorithm may yield systematic errors for~~
114 ~~anthropogenic emission sources located in different latitudes and under complex~~
115 ~~topographic and underlying surface conditions. The air mass factors (AMFs) used to~~
116 ~~convert~~~~yields one-step SO₂ slant column density (SCD) into VCD~~ are also subject to
117 ~~uncertainties.~~ ~~However, as~~ Fioletov et al. (2016) revealed an overall AMF uncertainty of
118 ~~28% which was created by surface reflectivity, surface pressure, ozone column, and cloud~~
119 ~~fraction. As Fioletov et al.~~ (2016) noted, the PCA retrieved SO₂ VCD was virtually derived
120 by ~~using~~~~adoption of an effective air mass factor (AMF) of 0.36 which is best applicable in~~
121 the summertime in the eastern United States (US). ~~The algorithm may cause systematic~~
122 ~~errors if anthropogenic emission sources are located in different latitudes and under~~
123 ~~complex topographic and underlying surface conditions. For instance, Wang (2014)~~
124 ~~suggested adopting~~ ~~has shown that~~ AMF \approx 0.57 in ~~the estimate of SO₂ VCD distribution in~~
125 eastern China. In the present study, we have ~~taken~~~~adopted~~ the AMFs values in China
126 provided by Fioletov et al. (2016) to adjust OMI measured VCD in the estimation of the
127 SO₂ emission ~~burden of the main~~~~major~~ point sources in northwestern China.

Formatted: Font color: Red

128 2.2 SO₂ monitoring, emission, and socioeconomic data

129 ~~— Figure 1 is a China map which highlights 6 provinces in northwestern China,~~
130 ~~including Shaanxi, Gansu, Qinghai, Ningxia, Xinjiang, and Inner Mongolia.~~
131 ~~Traditionally, Inner Mongolia is not classified as a northwestern province in China.~~
132 ~~Given that the most energy resources in Inner Mongolia are located in its western~~

133 ~~part of this province (Fig. 1), here we include this province in northwestern China.~~
134 ~~North China Plain (NCP), Beijing Tianjin Hebei (BTH), Yangtze River Delta (YRD),~~
135 ~~Pearl River Delta (PRD), and Sichuan Basin are also shown in the map.~~ To evaluate
136 and verify the spatial SO₂ VCD from OMI, ~~we collected~~ ground SO₂ monitoring data
137 of 2014 through 2015 at 188 sampling sites (cities) across China (~~Fig.~~**Figure 1**),
138 operated by the National Environmental Monitoring Center, available at
139 <http://www.aqistudy.cn/historydata>. ~~The statistics between OMI retrieved SO₂ VCD~~
140 ~~and monitored monthly and annually averaged SO₂ air concentrations during~~
141 ~~2014-2015 at 188 operational air quality monitoring stations across China are~~
142 ~~presented in Table S1 of Supplement. **Figure S1** is the correlation diagram between~~
143 ~~SO₂ VCD and sampled data. As shown in Table Annually averaged**S1** and **Fig. S1**,~~
144 ~~the OMI measured SO₂ VCDs agree well with the monitored ambient SO₂~~
145 ~~concentrations across China at the correlation coefficient of 0.85 (p<0.05) (**Table**~~
146 ~~**S1**). **Figure 2** further compared annually averaged SO₂ VCDs and SO₂ air~~
147 ~~concentrations from 2005 to 2015 in 6 capital cities in Urumqi (Xinjiang), Yinchuan~~
148 ~~(Ningxia), Beijing (BTH and NCP), Shanghai (YRD), Guangzhou (PRD), and~~
149 ~~Chongqing (Sichuan Basin), respectively. The mean SO₂ concentration data~~ were
150 collected from provincial environmental bulletin published by the Ministry of
151 Environmental Protection of China (MEPC)
152 (<http://www.zhb.gov.cn/hjzl/zghjzkgb/gshjzkgb>). ~~Results show that the annual~~
153 ~~variation of mean SO₂ VCDs match well with the monitored data except for Urumqi,~~
154 ~~the capital of Xinjiang Uygur Autonomous region. The OMI retrieved SO₂ VCDs in~~

155 ~~Shanghai and Chongqing are higher than the measured SO₂ concentrations from~~
156 ~~2010 to 2015 but the both show consistent temporal fluctuation and trend. The~~
157 ~~measured SO₂ concentrations peaked in 2013 in Yinchuan whereas the SO₂ VCD~~
158 ~~reached the peak in 2012 and decreased thereafter. OMI measured SO₂ VCDs in~~
159 ~~Urumqi show different yearly fluctuations compared with its annual concentrations.~~
160 ~~The measured SO₂ concentrations in Urumqi decreased from 2011 to 2015 whereas~~
161 ~~the OMI measured SO₂ VCDs did not illustrate obvious changes. It is not clear the~~
162 ~~causes leading to such the inconsistence. Measured concentrations might be subject~~
163 ~~to errors or not properly reported. Since the monitored SO₂ concentrations were~~
164 ~~collected in the urban area spatially averaged over 8 monitoring sites across the city~~
165 ~~whereas the OMI measured SO₂ VCD was averaged over all model grid points~~
166 ~~(0.25×0.25 latitude/longitude resolution) in Urumqi city. This could also result in the~~
167 ~~inconsistence between SO₂ VCD and measured data. However, such the error~~
168 ~~appeared not occurring in other cities.~~

169 ~~—~~ SO₂ anthropogenic emission inventory in China with a 0.25° longitude by 0.25°
170 latitude resolution for every two years from 2008 to 2012 was adopted from Multi
171 resolution Emission Inventory for China (MEIC) (Li et al., 2017, available at
172 <http://www.meicmodel.org>). ~~The comparison between annual OMI SO₂ VCD and~~
173 ~~SO₂ emissions in China is presented in Fig. 3. As shown, the annual variation in SO₂~~
174 ~~VCDs also agrees reasonably well with SO₂ emission data except for Midong. The~~
175 ~~OMI measured SO₂ VCD in the PRD and Sichuan Basin decreased from 2008 to~~
176 ~~2012.~~

Formatted: Adjust space between Latin and Asian text, Adjust space between Asian text and numbers

Formatted: Font: (Default) +Body (Calibri), 10.5 pt

Formatted: Default Paragraph Font, Font: (Default) +Body (Calibri), 10.5 pt

177 ~~___ but SO₂ emission changed little. Compared with the other five marked regions,~~
178 ~~the satellite measured SO₂ VCD in Midong declined in 2010 and inclined in 2012.~~
179 ~~However, SO₂ emissions in Midong increased in 2012 at about factor of 11 and 8~~
180 ~~higher than that in 2008 and 2010. It should be noted that the MEIC SO₂ emission~~
181 ~~inventory from the bottom-up approach might be subject to large uncertainties due to~~
182 ~~the lack of sufficient knowledge in human activities and emissions from different~~
183 ~~sources (Li et al., 2017; Zhao et al., 2011; Kurokawa et al., 2013). From this~~
184 ~~perspective, the satellite remote sensing provides a powerful tool in monitoring SO₂~~
185 ~~emissions from large point sources and the verification of emission inventories~~
186 ~~(Fioletov et al., 2016; Wang et al., 2015).—~~

187 —The socioeconomic data in China were collected from the China Statistical
188 Yearbooks and China Energy Statistical Yearbook, published by National Bureau of
189 Statistics of China (NBSC),
190 (<http://www.stats.gov.cn/tjsj/ndsj/>;[http://tongji.cnki.net/kns55/Navi/-](http://tongji.cnki.net/kns55/Navi/-HomePage.aspx?id=N2010080088&name=YCXME&floor=1)
191 [HomePage.aspx?id=N2010080088&name=YCXME&floor=1](http://tongji.cnki.net/kns55/Navi/-HomePage.aspx?id=N2010080088&name=YCXME&floor=1)), as well as China
192 National Environmental Protection Plan in the Eleventh Five-Years (2006-2010) and
193 Twelfth Five-Years (2011-2015) released by MEPC (<http://www.zhb.gov.cn>). These
194 data include industrial GDP, coal consumption, thermal power generation, steel
195 production, and SO₂ emission reduction plan, and they are presented in Table 1.

196 **2.3 Trends and step change**

197 The long-term trends of SO₂ VCD were estimated by linear regressions of the
198 gridded annually SO₂ VCD against their time sequence of 2005 through 2015. The

Formatted: Adjust space between Latin and Asian text, Adjust space between Asian text and numbers

199 gridded slopes (trends) of the linear regressions denote the increasing (positive) or
200 decreasing (negative) rates of SO₂ VCD (Wang et al., 2016; Huang et al., 2015;
201 Zhang et al., 2015, 2016).

202 The Mann-Kendall (MK) test was also employed in the assessments of the
203 temporal trend and step change point year of SO₂ VCD time series. The MK test is a
204 nonparametric statistical test (Mann,1945; Kendall, 1975), which is useful for
205 assessing the significance of trends in time series data (Waked et al., 2016; Fathian et
206 al., 2016). The MK test is often used to detect a step change point in the long term
207 trend of a time series dataset (Moraes et ~~al., al.~~ 1998; Li et al., 2016; Zhao et al.,
208 ~~2015, 2016~~). It is suitable for non-normally distributed data and censored data which
209 are not influenced by abnormal values (Yue and Pilon, 2004; Sharma et al. 2016; Yue
210 and Wang., 2004; Gao et al. 2016; Zhao et al., 2015). Recently, MK-test has also
211 been used in trend analysis for the time series of atmospheric chemicals, such as
212 persistent organic pollutants, surface ozone (O₃), and non-methane hydrocarbon
213 (Zhao et al., 2015; Assareh et al.,2016; Waked et al.,2016; Sicard et al., 2016). Here
214 the MK test was used to identify the temporal variability and step change point of
215 SO₂ VCD for 2005-2015 which may be associated with the implementation of the
216 national strategy and regulation in energy industry development and emission
217 control during this period. ~~of time~~. Under the null hypothesis (no trend), the test
218 statistic was determined using the following formula:

219
$$S_k = \sum_{i=1}^k r_i \quad (k= 2, 3, \dots, n) \quad (1)$$

220 where S_k is a statistic of the MK test, and

$$221 \quad r_i = \begin{cases} +1, (x_i > x_j) \\ 0, (x_i \leq x_j) \end{cases} \quad (j=1, 2, \dots, i-1) \quad (2)$$

222 where x_i is the variable in time series $x_1, x_2, \dots, x_i, r_i$ is the cumulative number for

223 $x_i > x_j$. The test statistic is normally distributed with a mean and variance is given by:

$$224 \quad E(S_k) = k(k-1)/4 \quad (3)$$

$$225 \quad Var(S_k) = \frac{k(k-1)(2k+5)}{72} \quad (4)$$

226 From these two equations, one can derive a normalized S_i , defined by

$$227 \quad UF_k = \frac{S_k - E(S_k)}{\sqrt{Var(S_k)}} \quad (k=1, 2, \dots, n) \quad (5)$$

228 where UF_k is the forward sequence, the backward sequence UB_k is calculated using

229 the same function but with the reverse data series such that $UB_k = -UF_k$.

230 In a two-sided trend test, a null hypothesis is accepted at the significance level if

231 $|UF_k| \leq (UF_k)_{1-\alpha/2}$, where $(UF_k)_{1-\alpha/2}$ is the critical value of the standard normal

232 distribution, with a probability of α . When the null hypothesis is rejected (i.e., when

233 any of the points in UF_k exceeds the confidence interval ± 1.96 ; $P=0.05$), a

234 ~~significantly significant~~ increasing or decreasing trend is determined. $UF_k > 0$ often

235 indicates an increasing trend, and vice versa. The test statistic used in the present

236 study enables us to discriminate the approximate time of trend and step change by

237 locating the intersection of the UF_k and UB_k curves. The intersection occurring within

238 the confidence interval $(-1.96, 1.96)$ indicates the beginning of a step change point

239 (Moraes et al., 1998; Zhang et al., 2011; Zhao et al., 2015).

240 2.4 Estimate of SO₂ emission from OMI measurements

241 To assess the connections between the major point sources in large-scale energy
 242 industrial bases in northwestern China and provincial emissions, we made use of OMI
 243 measured SO₂ VCD to inversely simulate the SO₂ emission from Ningdong Energy
 244 Chemical Industrial Base (NECIB) in Ningxia and Midong Energy Industrial Base
 245 (MEIB) in Xinjiang. McLinden et al. (2016) and Fioletov et al. (2015, 2016) have
 246 developed a source detection algorithm which fits OMI-measured SO₂ vertical
 247 column densities to a three-dimensional parameterization function of the horizontal
 248 coordinates and wind speed. This algorithm was employed in the present study to
 249 estimate the SO₂ source strength in the two industrial bases and its contribution to the
 250 provincial total SO₂ emissions. The details of this algorithm are referred to Fioletov et
 251 al (2015). Briefly, the source detection algorithm uses a Gaussian function $f(x, y)$
 252 multiplied by an exponentially modified Gaussian function $g(y, s)$ to fit the OMI SO₂
 253 measurements (Fioletov et al., 2015) $OMI_{SO_2} = a \cdot f(x, y) \cdot g(y, s)$, defined by

$$\begin{aligned}
 f(x, y) &= \frac{1}{\sigma_1 \sqrt{2\pi}} \exp\left(-\frac{x^2}{2\sigma_1^2}\right); \\
 g(y, s) &= \frac{\lambda_1}{2} \exp\left(\frac{\lambda_1(\lambda_1 \sigma^2 + 2y)}{2}\right) \cdot \operatorname{erfc}\left(\frac{\lambda_1 \sigma^2 + y}{\sqrt{2}\sigma}\right); \\
 \sigma_1 &= \begin{cases} \sqrt{\sigma^2 - 1.5y}, & y < 0; \\ \sigma, & y \geq 0 \end{cases}; \\
 \lambda_1 &= \lambda / s; \\
 \operatorname{erfc}(x) &= \frac{2}{\sqrt{\pi}} \int_x^\infty e^{-t^2} dt
 \end{aligned}
 \tag{6}$$

255 where x and y indicate the coordinates of the OMI pixel center (km); s is the wind
 256 speed (km h⁻¹) at the pixel center; a represents the total number of SO₂ molecules (or
 257 SO₂ burden) observed by OMI in a target emission source $\lambda = 1/\tau$, where τ is a

Field Code Changed

Field Code Changed

Field Code Changed

Field Code Changed

258 decay time of SO₂, and σ describes the width or spread of SO₂.

259 The $f(x, y)$ function represents the Gaussian distribution across the wind direction
260 line. The function $g(y, s)$ represents an exponential decay along the y -axis smoothed
261 by a Gaussian function. Once σ and τ are determined, the SO₂ burden as a function
262 of x, y , and s (OMI SO₂ (x, y, s)) can be reconstructed. SO₂ emission strength from a
263 large point source can be estimated by $E=a/\tau$. In the present study, following Fioletov
264 (2016) we choose a mean value of $\sigma=20$ km and $\tau=6$ h in the calculation of SO₂
265 emission large point sources of interested. Wind speed and direction on a $1^\circ \times 1^\circ$
266 latitude/longitude spatial resolution were collected from NCEP (National Centers for
267 Environmental Prediction) Final Operational Global Analysis
268 (<http://dss.ucar.edu/datasets/ds083.2/>). These data were interpolated to the location of
269 each OMI pixel center on a $1/4^\circ \times 1/4^\circ$ latitude/longitude spacing.

270 There are several potential sources of errors which need to be taken into account
271 when determining the overall uncertainty of the SO₂ emission estimation. Fioletov et
272 al. (2016) have highlighted three primary sources of errors in the OMI-based emission
273 estimates, including AMF, the estimation of the total SO₂ mass as determined from a
274 linear regression, and the selection of σ and τ used to fit OMI measurements. Based
275 on the coefficients of variation (CV, %) in these three error categories (McLinden et
276 al., 2014, 2016; Fioletov et al.; 2016) listed in **Table S1** of Supplement, we estimated
277 uncertainties in the SO₂ emissions derived from OMI measurements in the two major
278 point sources in northwestern China by running the source detection model repeatedly
279 for 10,000 times using Monte Carlo method. Results show the standard deviation of

280 -35 to 122 kt/yr for SO₂ emissions in NECIB and -29 to 95 kt/yr for SO₂ emissions in
281 MEIB from 2005 to 2015, respectively.

282 **2.5 Satellite data validation**

283 The OMI retrieved SO₂ PBL VCDs were evaluated by comparing with ambient
284 air concentration data of SO₂ from routine measurements by local official
285 operational air quality monitoring stations. The statistics between OMI retrieved SO₂
286 VCD and monitored annually averaged SO₂ air concentrations during 2014-2015 at
287 188 operational air quality monitoring stations across China are presented in **Table**
288 **S2** of Supplement. **Figure S1** is the correlation diagram between SO₂ VCD and
289 sampled data. As shown in **Table S2** and **Fig. S1**, the OMI measured SO₂ VCDs
290 agree well with the monitored ambient SO₂ concentrations across China at the
291 correlation coefficient of 0.85 (p<0.05) (**Table S2**). **Figure 2** further compares
292 annually averaged SO₂ VCD and SO₂ air concentrations from 2005 to 2015 in 6
293 capital cities. These are Urumqi, Yinchuan, Beijing, Shanghai, Guangzhou, and
294 Chongqing, respectively. The mean SO₂ concentration data were collected from
295 provincial environmental bulletin published by the Ministry of Environmental
296 Protection of China (MEPC) (<http://www.zhb.gov.cn/hjzl/zghjzkgb/gshjzkgb>).
297 Results show that the annual variation of mean SO₂ VCD are higher than the
298 measured SO₂ concentrations from 2010 to 2015, but SO₂ VCD match well with the
299 monitored data except for Urumqi, the capital of Xinjiang Uygur Autonomous
300 Region. The OMI retrieved SO₂ VCDs in Shanghai and Chongqing are higher than
301 the measured concentrations in these two regions show consistent temporal

302 fluctuation and trend. The measured SO₂ concentrations peaked in 2013 in Yinchuan
303 whereas the SO₂ VCD reached the peak in 2012 and decreased thereafter. OMI
304 measured SO₂ VCD in Urumqi shows different yearly fluctuations compared with its
305 annual concentrations. The measured SO₂ concentrations in Urumqi decreased from
306 2011 to 2015 whereas the OMI measured SO₂ VCD did not illustrate obvious
307 changes. In particular, the monitored mean SO₂ concentration from 2013 to 2015
308 decreased by 75% compared with that from 2005 to 2012. This is partly attributed to
309 the change in air quality monitoring sites in Urumqi city. Before 2013, there were
310 only three operational air quality sites in Urumqi City, all located in the heavily
311 polluted downtown region. Since 2013, the air monitoring sites increased from 3 to 7.
312 The four new sites are located in less polluted suburbs of the city. As a result, the
313 spatially averaged SO₂ concentrations over 3 downtown air quality monitoring sites
314 before 2013 were higher than the mean concentrations averaged over 7 monitoring
315 sites (http://xjny.ts.cn/content/2012-06/05/content_6899388.htm). It is worth noting
316 that the measured SO₂ concentration in Urumqi is the highest among all cities as
317 shown in Fig. 2 whereas the OMI VCD value in Urumqi was lower than other
318 selected cities. This may be due to systematic biases in OMI-retrieved SO₂ VCD. In
319 the present study, the level 3 OMI PBL SO₂ VCD data produced by the PCA
320 retrievals were used to estimate the spatiotemporal variation in SO₂ pollution in
321 China. The PCA retrievals have a negative bias over some highly reflective surfaces
322 in arid and semi-arid lands, such as many some places in the Sahara (up to about -0.5
323 DU in monthly mean VCD)

324 <https://disc.gsfc.nasa.gov/Aura/data-holdings/OMI/documents/v003/omso2readme->
325 [v120-20140926.pdf](https://disc.gsfc.nasa.gov/Aura/data-holdings/OMI/documents/v003/omso2readme-v120-20140926.pdf)). Also, PCA retrievals is subject to the systematic bias of 0.7-0.9
326 DU in relatively high latitude regions. Located at a relatively high latitude in
327 northwestern China with a large surrounding area covered by Gobi desert, the PCA
328 algorithm might yield lower SO₂ VCD value in Urumqi than other cities shown in
329 **Fig. 2.**

330 SO₂ emissions data were further collected to compare with annual OMI SO₂
331 VCD in selected regions. The results are presented in **Fig. 3.** As shown, the annual
332 variation in SO₂ VCD agrees reasonably well with SO₂ emission data except for
333 Urumqi-Midong region. The OMI measured SO₂ VCD in the PRD and Sichuan Basin
334 decreased from 2008 to 2012, but SO₂ emission changed little. Compared with the
335 other five marked regions (**Fig. 1**), the satellite measured SO₂ VCD in
336 Urumqi-Midong declined in 2010 and inclined in 2012. However, SO₂ emissions in
337 Urumqi-Midong 2012 are factors of 11 and 8 higher than that in 2008 and 2010,
338 respectively. It should be noted that air pollutants released in the atmosphere are
339 affected by physical and chemical processes. They may be transported over large
340 distances by atmospheric motions, transformed into other compounds by chemical or
341 photochemical processes, and "washed out" or deposited at the Earth's surface (Zhao
342 et al., 2017; Brasseur et al., 1998). The atmospheric removal and advection processes
343 may also contribute to the inconsistency between monitored and satellite observations.
344 In addition, the MEIC SO₂ emission inventory from the bottom-up approach might be
345 subject to large uncertainties due to data manipulation, and the lack of sufficient

346 knowledge in human activities and emissions from different sources (Li et al., 2017;
347 Zhao et al., 2011; Lu et al., 2011; Kurokawa et al., 2013). The uncertainties in the
348 MEIC estimated SO₂ emissions used in the present study are up to ±12% (Li et al.,
349 2017). As shown in Fig. 3, the OMI measured SO₂ VCD from 2008 to 2012 in
350 Urumqi-Midong was about 0.2 DU which was comparable with that in the EGT.
351 However, the reported SO₂ emission in Urumqi-Midong was only 4% of the SO₂
352 emission in the EGT in 2012 and 0.5% of that in the EGT from 2008 to 2010. It might
353 be subject to that part large SO₂ emission sources were not included in emission
354 inventory. From this perspective, the satellite remote sensing provides a very useful
355 tool in monitoring SO₂ emissions from large point sources and in the verification of
356 emission inventories (Fioletov et al., 2015, 2016; McLinden et al., 2016; Wang et al.,
357 2015;).

359 **3 Results and discussion**

360 **3.1. Spatiotemporal variation in OMI measured SO₂ in China**

361 Given higher population density and stronger industrial activities, eastern and
362 southern China are traditionally industrialized and heavily contaminated regions by
363 air pollutions and acid rains caused by SO₂ emissions. **Figure 4a** shows annually
364 averaged OMI SO₂ VCD over China on a 0.25° × 0.25° latitude/longitude
365 resolution averaged from 2005 to 2015. SO₂ VCD was higher considerably in eastern
366 and central China, and Sichuan Basin than that in northwestern China. The highest
367 SO₂ VCD was found in the NCP, including Beijing-Tianjin-Hebei (BTH), Shandong,

Formatted: Font: Not Superscript/
Subscript

368 and Henan province. The annually averaged SO₂ VCD between 2005-2015 in this
369 region reached 1.36 DU. This result is in line with previous satellite remote sensing
370 retrieved SO₂ emissions in eastern China (Krotkov et al 2016; Lu et al., 2010;
371 Bauduin et al., 2016; Jiang et al 2012; Yan et al., 2014). However, in contrast to the
372 spatial distribution of decadal mean SO₂ VCD (**Fig. 4a**), the slopes of the linear
373 regression relationship between annual average OMI-retrieved SO₂ VCD and the
374 time sequence from 2005 to 2015 over China show that the negative trends
375 overwhelmed industrialized eastern and southern China, particularly in the NCP,
376 Sichuan Basin, the YRD, and PRD, manifesting significant decline of SO₂ emissions
377 in these regions. SO₂ VCD in the PRD exhibited the largest decline at a rate of 7%
378 yr⁻¹, followed by the NCP (6.7% yr⁻¹), Sichuan Basin (6.3% yr⁻¹), and the YRD (6%
379 yr⁻¹), respectively. Annual average SO₂ VCD in the PRD, NCP, Sichuan Basin, and
380 YRD decreased by 52%, 50% , 48%, and 46% in 2015 compared to 2005 (**Fig. 5**),
381 though the annual fluctuation of SO₂ VCD shows rebounds in 2007 and 2011 which
382 are potentially associated with the economic resurgence stimulated by the central
383 government of China (He et al., 2009; Diao et al., 2012). The reduction of SO₂ VCD
384 after 2011 in these regions reflects virtually the response of SO₂ emissions to the
385 regulations in the reduction of SO₂ release, the mandatory application of the flue-gas
386 desulfurization (FGD) on coal-fired power plants and heavy industries, and the
387 slowdown in the growth rate of the Chinese economy (CSC, 2011a; Wang et al.,
388 2015, Chen et al., 2016).

389 ~~Since~~ ~~As also shown in Fig. 4b, in contrast to widespread decline of SO₂~~

390 ~~VCD, there are two "hot spots" featured by moderate increasing trends of SO₂ VCD,~~
391 ~~located in the China's Energy Golden Triangle (EGT, Shen et al., 2016, Ma and Xu,~~
392 ~~2017) and Urumqi-Midong regions in northwestern China. The annual growth rate of~~
393 ~~SO₂ VCD from 2005 to 2015 are 3.4% yr⁻¹ in the EGT and 1.8% yr⁻¹ in~~
394 ~~Urumqi-Midong, respectively (Fig. 4b). Further details are presented in Table 1.~~
395 ~~SO₂ VCDs in these two regions peaked in 2011 and 2013 which were 1.6 and 1.7~~
396 ~~times of that in 2005 (Fig. 5). The raising SO₂ VCDs in the part of the EGT have~~
397 ~~been reported by Shen et al. (2016). The second hot spot is located in Midong~~
398 ~~industrial park, about 40 km away from Urumqi, the capital of the Xinjiang Uygur~~
399 ~~Autonomous Region. The both EGT and Midong industrial parks are featured by~~
400 ~~extensive coal mining, thermal power generation, coal chemical, and coal~~
401 ~~liquefaction industries. The reserve of coal, oil and natural gas in the EGT is~~
402 ~~approximately 1.05×10¹² ton of standard coal equivalent, accounting for 24% of the~~
403 ~~national total energy reserve in China (CRGECR, 2015). It has been estimated that~~
404 ~~there are deposits of 20.86 billion tons of oil, 1.03 billion cubic meters of natural gas,~~
405 ~~and 2.19 trillion tons of coal in Xinjiang, accounting for 30%, 34% and 40% of the~~
406 ~~national total (Dou, 2009). Over the past decades, a large number of energy-related~~
407 ~~industries have been constructed in northwestern China, such as the EGT and~~
408 ~~Midong chemical industrial parks in order to enhance China's energy security in the~~
409 ~~21st century and speed up local economy. Rapid development of energy and coal~~
410 ~~chemical industries in Ningxia Hui Autonomous region and Xinjiang of~~
411 ~~northwestern China alone resulted in the significant demands to coal mining and coal~~

412 ~~products. The coal consumption, thermal power generation, and the gross industrial~~
413 ~~output increased by 2.7, 3.5, and 6.6 times in Ningxia from 2005 to 2015, and by 2.7,~~
414 ~~4.2 and 6.6 times in Xinjiang during the same period (NBSC, 2005, 2015). As a~~
415 ~~result, SO₂ emissions increased markedly in these regions, as shown by the~~
416 ~~increasing trends of SO₂ VCD in the EGT and Midong (Fig. 4b). Figure 6 illustrates~~
417 ~~the fractions of OMI measured annual SO₂ VCD and SO₂ emissions averaged over~~
418 ~~the 6 provinces of northwestern China in the annual national total VCD (Fig. 6a) and~~
419 ~~emissions (Fig. 6b) from 2005 to 2015. The both SO₂ VCD and emission fractions in~~
420 ~~northwestern China in the national total increased over the past decade. By 2015, the~~
421 ~~mean SO₂ VCD fraction in 6 northwestern provinces has reached 38% in the national~~
422 ~~total. The mean emission fraction was about 20% in the national total. It should be~~
423 ~~noted that there were large uncertainties in provincial SO₂ emission data which often~~
424 ~~underestimated SO₂ emissions from major point sources (Li et al., 2017; Han et al.,~~
425 ~~2007). In this sense, OMI retrieved SO₂ VCD fraction provides a more reliable~~
426 ~~estimate to the contribution of SO₂ emission in northwestern China to the national~~
427 ~~total.~~

428 ~~— The annual percentage changes in SO₂ VCD from 2005 onward are consistent~~
429 ~~well with per capita SO₂ emissions in China (Fig. 7). As aforementioned, while the~~
430 ~~annual total SO₂ emissions in the well developed BTH, YRD, and PRD were higher~~
431 ~~than that in northwestern provinces, the per capita emissions in all provinces of~~
432 ~~northwestern China, especially in Ningxia and Xinjiang, were about factors of 1 to 6~~
433 ~~higher than that in the BTH, YRD, and PRD, as shown in Fig. 7. In contrast to~~

434 ~~declining annual emissions from the BTH, YRD, and PRD, the per capita SO₂~~
435 ~~emissions in almost all western provinces have been growing from 2005 onward.~~—

436 **3.2 Trend and step changes in OMI measured SO₂ by MK test**

437 ~~— Given that~~ in the MK test the signs and fluctuations of UF_k are often used to
438 predict the trend of a time series, this approach is further applied to quantify the trends
439 and step changes in annually SO₂ VCD time series in those highlighted regions (a-f)
440 in **Fig. 4b** from 2005 to 2015. Results are illustrated in **Fig. 6.8**. As shown, the
441 forward and backward sequences UF_k and UB_k intersect at least once from 2005 to
442 2015. These intersections are all well within the confidence levels between -1.96 and
443 1.96 at the statistical significance $\alpha=0.01$. A common feature of the forward sequence
444 UF_k in eastern and southern China provinces is that UF_k has been declining and
445 become negative from 2007 to 2009 onward (**Fig. 6a-d, 8a-d**), confirming the
446 downturn of SO₂ atmospheric emissions and levels in these industrialized and well
447 ~~developed regions in China. In the EGT and Midong areas of northwestern China (Fig.~~
448 ~~4b), however, the UF_k values for SO₂ VCD are positive and growing, illustrating clear~~
449 ~~upward trends of SO₂ VCD over these two large scale energy industry parks,~~
450 ~~revealing the response of SO₂ emissions to the energy industry relocation and~~
451 ~~development in northwestern China. To guarantee the national energy security and to~~
452 ~~promote the regional economy, the EGT energy program has been accelerating since~~
453 ~~2003 under the national energy development and relocation plan (Zhu and Ruth, 2015;~~
454 ~~Chen et al., 2016), characterized by the rapid expansion of the Ningdong energy and~~
455 ~~chemical industrial base (NECIB) which is located about 40 km away from Yinchuan,~~

456 ~~the capital of Ningxia (Shen et al., 2016). By the end of 2010, a large number of coal~~
457 ~~chemical industries, including the world largest coal liquefaction and thermal power~~
458 ~~plants, have been built and operated, and the total installed capacity of thermal power~~
459 ~~generating units has reached 1.47 million kilowatts (Zhao, 2016).~~ developed regions
460 in China. The step change points of OMI measured SO₂ VCDs ~~Under the same~~
461 ~~national plan, the Midong industrial park in Xinjiang started to construction and~~
462 ~~operation from the early to mid-2000s which has almost the same industrial structures~~
463 ~~as those in the EGT, featured by coal fired power generation, coal chemical industry,~~
464 ~~and coal liquefaction.~~
465 ~~— For those regions with declining trends of SO₂ VCD, their step change points~~
466 the NCP, YRD and Sichuan Basin occurred between 2012 and 2013. These step
467 change points coincide with the implementation of the new Ambient Air Quality
468 Standard in 2012, which set a lower ambient SO₂ concentration limit in the air (MEPC,
469 2012), and the Air Pollution Prevention and Control Action Plan in 2013 by the State
470 Council of China (CSC, 2013a). This Action Plan requests to take immediate actions
471 to control and reduce air pollution in China, including cutting down industrial and
472 mobile emission sources, adjusting industrial and energy structures, and promoting
473 the application of clean energy in the BTH, YRD, PRD and Sichuan Basin. The step
474 change in SO₂ VCD over the PRD occurred in the earlier year of 2009-2010 and from
475 this period onward the decline of SO₂ VCD speeded up, as shown by the forward
476 sequence UF_k which became negative since 2007 and was below the confidence level
477 of -1.96 after 2009, suggesting significant decreasing VCD from 2009 (**Fig. 6c, 8e**).

478 In April 2002, the Hong Kong Special Administrative Region (HKSAR) Government
479 and the Guangdong Provincial Government reached a consensus to reduce, on a best
480 endeavor basis, the anthropogenic emissions of SO₂ by 40% in the PRD by 2010,
481 using 1997 as the base year
482 (http://www.epd.gov.hk/epd/english/action_blue_sky/files/exsummary_e.pdf). By the
483 end of 2010, all thermal power units producing more than 0.125 million kilowatts
484 electricity in the PRD were equipped with the FGD. During the 11th Five-Year Plan
485 (2006-2010), the thermal power units with 1.2 million kilowatts capacity have been
486 shut down. SO₂ emission was reduced by 18% in 2010 compared to that in 2005
487 (NBSC, 2006, 2011). This likely caused the occurrence of the step change in SO₂
488 VCD over 2009-2010.

489 **3.2. OMI measured SO₂ "hot spots" in northwestern China**

490 As also shown in Fig. 4b, in contrast to widespread decline of SO₂ VCD, there
491 are two "hot spots" featured by moderate increasing trends of SO₂ VCD, located in
492 the China's Energy Golden Triangle (EGT, Shen et al., 2016, Ma and Xu, 2017) and
493 Urumqi-Midong region in northwestern China. The annual growth rate of SO₂ VCD
494 from 2005 to 2015 are 3.4% yr⁻¹ in the EGT and 1.8% yr⁻¹ in Urumqi-Midong,
495 respectively (Fig. 4b). SO₂ VCD in these two regions peaked in 2011 and 2013
496 which were 1.6 and 1.7 times of that in 2005 (Fig. 5). The raising SO₂ VCD in the
497 part of the EGT have been reported by Shen et al. (2016). The second hot spot is
498 located in Urumqi-Midong region including MEIB that is about 40 km away from
499 Urumqi. The both EGT and MEIB are featured by extensive coal mining, thermal

500 power generation, coal chemical, and coal liquefaction industries. The reserve of
501 coal, oil and natural gas in the EGT is approximately 1.05×10^{12} ton of standard coal
502 equivalent, accounting for 24% of the national total energy reserve in China
503 (CRGECR, 2015). It has been estimated that there are deposits of 20.86 billion tons
504 of oil, 1.03 billion cubic meters of natural gas, and 2.19 trillion tons of coal in
505 Xinjiang, accounting for 30%, 34% and 40% of the national total (Dou, 2009). Over
506 the past decades, a large number of energy-related industries have been constructed
507 in northwestern China, such as the EGT and MEIB to enhance China's energy
508 security in the 21st century and speed up the local economy. The rapid development
509 of energy and coal chemical industries in Ningxia Hui Autonomous Region and
510 Xinjiang of northwestern China alone resulted in the significant demands to coal
511 mining and coal products. The coal consumption, thermal power generation, and the
512 gross industrial output increased by 2.7, 3.5, and 6.6 times in Ningxia from 2005 to
513 2015, and by 2.7, 4.2 and 6.6 times in Xinjiang during the same period (NBSC, 2005,
514 2015). As a result, SO₂ emissions increased markedly in these regions, as shown by
515 the increasing trends of SO₂ VCD in the EGT and Urumqi-Midong region (Fig. 4b).

516 The MK forward sequence further confirms the increasing SO₂ VCD in the EGT
517 and Urumqi-Midong. As seen in Fig. 6e and 6f, the UF_k values for SO₂ VCD are
518 positive and growing, illustrating clear upward trends of SO₂ VCD over these two
519 large-scale energy industry bases, revealing the response of SO₂ emissions to the
520 energy industry relocation and development in northwestern China. To guarantee the
521 national energy security and to promote the regional economy, the EGT energy

522 program has been accelerating since 2003 under the national energy development and
523 relocation plan (Zhu and Ruth, 2015; Chen et al., 2016), characterized by the rapid
524 expansion of the NECIB which is located about 40 km away from Yinchuan, the
525 capital of Ningxia (Shen et al., 2016). By the end of 2010, a large number of coal
526 chemical industries, including the world largest coal liquefaction and thermal power
527 plants, have been built and operated, and the total installed capacity of thermal power
528 generating units has reached 1.47 million kilowatts (Zhao, 2016). Under the same
529 national plan, the MEIB in Xinjiang started to construction and operation from the
530 early to mid-2000s which have almost the same industrial structures as those in the
531 EGT, featured by coal-fired power generation, coal chemical industry, and coal
532 liquefaction.

533 The statistical significant step change points of SO₂ VCD in the EGT and
534 Urumqi-Midong took place in 2006 and 2009 (Fig. 6e and 6f), differing from those
535 regions with decreasing trends of SO₂ VCD in eastern and southern China. The first
536 step change point in 2006-2007 corresponds to the increasing SO₂ emissions in these
537 two large-scale energy bases till their respective peak emissions in EGT (2007) and
538 Urumqi-Midong (2008). The second step change point in 2009 coincides with the
539 global financial crisis in 2008 which slowed down considerably the economic growth
540 in 2009 in China, leading to raw material surplus and the remarkable reduction in the
541 demand ~~forte~~ coal products.

542 **3.3 OMI SO₂ time series and step change point year in northwestern China**

543 The clearly visible "hot spots" featured by increasing OMI measured SO₂ VCD

544 in the EGT/NECIB and MEIB raise a question: to what extent could these
545 large-scale energy industrial bases affect the trend and fluctuations of SO₂ emissions
546 in northwestern China? **Figure 7** illustrates the fractions of OMI measured annual
547 SO₂ VCD and SO₂ emissions averaged over the 6 provinces of northwestern China
548 in the annual national total VCD (**Fig. 7a**) and emissions (**Fig. 7b**) from 2005 to
549 2015. The both SO₂ VCD and emission fractions in northwestern China in the
550 national total increased over the past decade. By 2015, the mean SO₂ VCD fraction
551 in 6 northwestern provinces has reached 38% in the national total. The mean
552 emission fraction was about 20% in the national total. It should be noted that there
553 were large uncertainties in provincial SO₂ emission data which often underestimated
554 SO₂ emissions from major point sources (Li et al., 2017; Han et al., 2007). In this
555 sense, OMI retrieved SO₂ VCD fraction provides a more reliable estimate to the
556 contribution of SO₂ emission in northwestern China to the national total.

557 The annual percentage changes in SO₂ VCD from 2005 onward are consistent
558 well with the per capita SO₂ emissions in China (**Fig. 8**). As aforementioned, while
559 the annual total SO₂ emissions in the well-developed BTH, YRD, and PRD were
560 higher than that in northwestern provinces, the per capita emissions in all provinces
561 of northwestern China, especially in Ningxia and Xinjiang where the NECIB and
562 MEIB are located, were about factors of 1 to 6 higher than that in the BTH, YRD,
563 and PRD, as shown in **Fig. 8**. In contrast to declining annual emissions from the
564 BTH, YRD, and PRD, the per capita SO₂ emissions in almost all western provinces
565 have been growing from 2005 onward.

566 Since almost all large-scale coal chemical, thermal power generation, and coal
567 liquefaction industries were built in energy-abundant and sparsely populated
568 northwestern China over the past two decades, particularly since the early 2000s,
569 those large-scale industrial ~~parks and~~ bases in this part of China likely play an
570 important role in the growing SO₂ emissions in northwestern provinces. We further
571 examine the OMI retrieved SO₂ VCD to confirm and evaluate the changes in SO₂
572 emissions in northwestern China which should otherwise respond to these
573 large-scale energy programs under the national plan for energy relocation and
574 expansion. **Figure 9** displays the MK test statistics for SO₂ VCD in the 6 provinces
575 in northwestern China from 2005-2015. The forward sequence UF_k suggests
576 decreasing trends in Shaanxi and Gansu provinces and a moderate increase in
577 Qinghai province. In Xinjiang and Ningxia where the most energy industries were
578 relocated and developed for the last decade (2005-2015), as aforementioned, UF_k
579 time series estimated using SO₂ VCD data illustrate clear upward trends. Compared
580 with those well-developed regions in eastern and southern China, the UF_k values of
581 SO₂ VCD in these northwestern provinces are almost all positive, except for Shaanxi
582 province where the UF_k turned to negative from 2008, and Gansu province where
583 the UF_k value become negative during 2012-2013.

584 -The step change points identified by the MK test for SO₂ VCD in northwestern
585 China appear associated strongly with the development and use of coal energy. As
586 shown in **Fig. 9**, the intersection of the forward and backward sequences UF_k and
587 UB_k within the confidence levels of -1.96 (straight green line) to 1.96 (straight

588 purple line) can be identified in 2006 and 2007 in Ningxia and Xinjiang, respectively,
589 corresponding well to the expansion of two largest energy industry bases from 2003
590 onward in Ningxia (NECIB) and ~~Midong energy industry park in~~ Xinjiang (MEIB).
591 The step change point of SO₂ VCD in 2012 in Gansu province coincides with
592 fuel-switching from coal to gas in the capital city (Lanzhou) and many other places
593 of the province initiated from 2012 (CSC, 2013b). The MK derived step change
594 point in Shaanxi province ~~occurred~~ occurred in 2010 which ~~was~~ was a clear signal of
595 marked decline of fossil fuel products in northern Shaanxi where, as the part of the
596 EGT (Ma and Xu, 2017) of China, the largest energy industry base in the province is
597 located, right after the global financial crisis.

598 It is interesting to note that the forward sequences UF_k of SO₂ VCD (**Fig. 9e** and
599 **f**) in Ningxia and Xinjiang exhibit the similar fluctuations as that in Ningdong
600 (NECIB) and ~~Urumqi-Midong (MEIB) energy industrial bases~~ (Fig. ~~9e~~ **8e** and **f**),
601 manifesting the potential associations between the SO₂ emissions in these two
602 large-scale energy industrial ~~bases~~ **spark**s (major point sources) and provincial
603 emissions in Ningxia and Xinjiang, respectively. This suggests that large-scale energy
604 industrial ~~parks and~~ **spark**s might likely overwhelm or play an important role in the
605 SO₂ emissions in those energy-abundant provinces in northwestern China. ~~To assess~~
606 ~~the connections between the major point sources in the two energy industrial parks~~
607 ~~and the provincial emissions, we made use of OMI measured SO₂ VCD to inversely~~
608 ~~simulate the SO₂ emission burdens in Xinjiang and Ningxia. We used the source~~
609 ~~detection algorithm (McLinden et al., 2016) and the approach, which fits~~

610 ~~OMI measured SO₂ vertical column densities to a three-dimensional parameterization~~
611 ~~function of the horizontal coordinates and wind speed, proposed by Fioletov et al.~~
612 ~~(2015, 2016), to estimate the SO₂ source strength in the two industrial parks and its~~
613 ~~contribution to the provincial total SO₂ burdens.~~ **Figure 10** illustrates mean SO₂
614 ~~VCD~~ burdens from 2005 to 2015 in northern Xinjiang (**Fig. 10a**) and Ningxia (**Fig.**
615 **10b**). The largest ~~concentrations~~ burdens can be seen clearly in the ~~MEIB~~ Midong
616 ~~energy industrial base~~ and the NECIB in these two minority autonomous regions of
617 China. Lower SO₂ ~~concentration~~ ~~emission~~ burdens are illustrated in mountainous
618 areas of northern Xinjiang. ~~Based on inverse modeling~~ **Figure 11** illustrates the annual
619 ~~variations~~ of ~~estimated~~ SO₂ ~~emission~~ burdens ($a \cdot 10^{26}$ molecules) in the ~~source~~
620 ~~detection model (section 2.4), we estimated SO₂ emission (E , kt yr⁻¹) in the~~ NECIB
621 and ~~MEIB from 2005 to 2015, defined by $E = a/\tau$, where τ is a decay time of SO₂~~
622 ~~(section 2.4).~~ Midong energy industrial parks (scaled on the left Y axis) and their
623 respective fractions (% , scaled on the right Y axis) in the total provincial SO₂ burdens
624 in Ningxia and Xinjiang, respectively. ~~The results are illustrated in Fig. 11. As shown,~~
625 ~~the SO₂ emission~~ SO₂ burden increased from 2005 and reached the maximum in 2011
626 in the NECIB and declined thereafter, in line with the annual SO₂ VCD fluctuations
627 (**Fig. 5**) in this ~~energy industry base~~ industrial park which is, as aforementioned,
628 attributable to the economic rebound in 2011 in China. Of particular interest is the
629 large fractions of the estimated SO₂ emission burden in the NECIB in Ningxia
630 ~~Province (Fig. 11a) from 2005 to 2015. These large fractions suggest, showing~~ that
631 this ~~energy industry~~ industrial park alone contributed up to ~~more than about 40–50%~~

Formatted

Formatted: Font color: Red

Formatted: Font:

Formatted: Font:

Formatted: Font:

Formatted: Font:

Formatted: Font: Not Superscript/
Subscript

Formatted: Font:

Formatted: Font:

632 emission ~~burdens~~ to the provincial total SO₂ emission ~~burden~~. Likewise, the OMI
633 SO₂ VCD derived SO₂ emissions~~SO₂ emission burden enhanced from 2005 and~~
634 ~~peaked in the MEIB also made an appreciable contribution (15-20%)~~2013 in Midong
635 energy industrial park (**Fig. 11b**). The emission burden in this park contributed about
636 ~~25-35%~~ to the provincial total SO₂ emission in Xinjiang~~burden~~. Compared with the
637 NECIB, the SO₂ emission burden is higher in the Midong industrial park but has the
638 ~~lower fraction in the provincial total emission burden~~. Covered by a large area of Gobi
639 desert ~~and Gobi~~ (Junngar Basin), ~~underlying surfaces~~, there are only a few of SO₂
640 emission sources in vast northern Xinjiang region (total area of Xinjiang is 1.66×10^6
641 km²). This likely leads to the small fractions of SO₂ emissions in the MEIB in the total
642 SO₂ emission in Xinjiang. **Figure 11c** and **11d** show SO₂ VCDs (the left y-axis) and
643 the ratios (the right y-axis) of the mean VCDs in NECIB and MEIB to the provincial
644 mean VCDs in Ningxia and Xinjiang from 2005 to 2015, respectively. It can be seen
645 that the maximum mean SO₂ VCD over the MEIB is about a factor of 4.5 greater than
646 the mean SO₂ VCD over Xinjiang province (Fig. 11d). This ratio is larger than the
647 ratio (2.9) of the SO₂ VCD in the NECIB to the SO₂ VCD averaged over Ningxia
648 province (Fig. 11c).~~km²~~, leading to the small ratio of the major point source (Midong)
649 ~~to total emission sources in Xinjiang~~. Nevertheless, overall our results manifest that,
650 although there were only a small number of SO₂ point sources in these two energy
651 industrial ~~bases~~parks, the SO₂ emissions from the NECIB and MEIB~~se parks~~ made
652 significant contributions to provincial total emissions. Given that the national strategy
653 for China's energy expansion and safety during the 21st century is, to a large extent, to

654 | develop large-scale energy ~~industry bases~~industrial parks in northwestern China,
655 | particularly in Xinjiang and Ningxia (Zhu and Ruth, 2015; Chen et al., 2016) where
656 | the energy resources are most abundant in China, we would expect that the rising SO₂
657 | emissions in northwestern China would increasingly be attributed to those large-scale
658 | energy ~~industry bases~~industrial parks and contributed ~~increasingly~~ to the national total
659 | SO₂ emission in China.

660 | **Table 1** presents the annual average growth rates of SO₂ VCD, industrial
661 | (second) Gross Domestic Product (GDP), and major coal-consuming industries in
662 | northwestern China and three developed areas (BTH, YRD, PRD) in eastern and
663 | southern China. The positive growth rates of SO₂ VCD can be observed in the three
664 | ~~provinces~~ and autonomous regions (Qinghai, Ningxia, and Xinjiang) of northwestern
665 | China. Although the growth rates of SO₂ VCD in other two provinces (Gansu and
666 | Shaanxi) are negative, the magnitudes of the negative growth rates are smaller than
667 | those in the BTH, YRD, and PRD, except for Zhejiang province in the YRD. This
668 | regional contrast reflects both their economic and energy development activities, and
669 | the SO₂ emission control measures implemented by the local and central
670 | governments of China. Although China has set a national target of 10% SO₂
671 | emission reduction (relative to 2005) during 2006-2010 and 8% (relative to 2010)
672 | during 2011-2015 (CSC, 2007; CSC, 2011b), under the Grand Western Development
673 | Program of China, the regulation for SO₂ emission control was waived in those
674 | energy-abundant provinces of northwestern China in order to speed up the large-
675 | scale energy industrial bases and local economic development, and improve local

676 | personal income. ~~Also, In addition,~~ although FGDs were widely installed in
677 | coal-fired power plants and other industrial sectors since the 1990s, by 2010 as much
678 | as 57% of these systems were installed in eastern and southern China (Zhao et al.,
679 | 2013). The capacity of small power generators which were shut-down in western
680 | China was merely about 10808 MW, only accounting for about 19% of the capacity
681 | of total small power plants which were eliminated in China (55630 MW) during the
682 | 11th Five-Year Plan period (2006-2010) (Cui et al., 2016). As shown in **Table 1**, the
683 | SO₂ emission reduction plans virtually specified the zero percentage of SO₂ emission
684 | reductions in Qinghai, Gansu, and Xinjiang and lower reduction percentage in the
685 | emission reduction in Ningxia and Inner Mongolia as compared to eastern and
686 | southern China during the 11th (2006-2010) and 12th (2011-2015) Five-Year Plan.
687 | As a result, the average growth rate for thermal power generation, steel production,
688 | and coal consumption from 2005 to 2015 in northwestern China reached 14.1% yr⁻¹,
689 | 35.7% yr⁻¹, and 11.9% yr⁻¹, considerably higher than the averaged growth rates over
690 | eastern and southern China (5.9% yr⁻¹ in the BTH, 0.8% yr⁻¹ in the YRD, and 2.3%
691 | yr⁻¹ in the PRD).

692

693 **4 Conclusions**

694 | The spatiotemporal variation in SO₂ concentration during 2005-2015 over
695 | China was investigated by making use of the PBL SO₂ column concentrations
696 | measured by the ~~OMI Ozone Monitoring Instrument~~. The highest SO₂ VCD was
697 | found in the NCP, the most heavily polluted area by SO₂ ~~and particular matters (PM)~~

698 in China, including Beijing-Tianjin-Hebei, Shandong, and Henan province. Under
699 the national regulation for SO₂ control and emission reduction, the SO₂ VCD in
700 eastern and southern China underwent widespread decline during this period.
701 However, the OMI measured SO₂ VCD detected two "hot spots" in the EGT
702 (Ningxia-Shaanxi-Inner Mongolia) and Midong (Xinjiang) energy industrial
703 ~~bases.parks~~, in contrast to the declining SO₂ emissions in eastern and southern China,
704 displaying an increasing trend with the annual growth rate of 3.4% yr⁻¹ in the EGT
705 and 1.8% yr⁻¹ in Midong, respectively. The trend analysis further revealed enhanced
706 SO₂ emissions in most provinces of northwestern China likely due to ~~the~~ national
707 strategy for energy industry expansion and relocation in energy-abundant
708 northwestern China. As a result, per capita SO₂ emission in northwestern China has
709 exceeded industrialized and populated eastern and southern China, making
710 increasing contributions to the national total SO₂ emission. The estimated SO₂
711 ~~emissions~~~~burdens~~ in the Ningdong (Ningxia) and Midong (Xinjiang) energy
712 industrial ~~bases.parks~~ from OMI measured SO₂ VCD showed that the SO₂ emissions
713 in these two industrial ~~bases.parks~~ made significant contributions to the ~~total~~
714 provincial ~~total~~-emissions. This indicates, on one side, that the growing SO₂
715 emissions in northwestern China would increasingly come from those large scale
716 energy industrial ~~bases.parks~~ under the national energy development and relocation
717 plan. On the other side, this fact also suggests that it is likely more straightforward to
718 control and reduce SO₂ emissions in northwestern China because the SO₂ control
719 measures could be readily implemented and authorized in those state-owned

720 large-scale energy industrial bases.

721

722 **The Supplement related to this article is available online**

723 *Acknowledgements.* This work is supported by the National Natural Science
724 Foundation of China (grants 41503089, 41371478, and 41671460), Gansu Province
725 Science and Technology Program for Livelihood of the People (1503FCMA003), the
726 Natural Science Foundation of Gansu Province of China (1506RJZA212), and
727 Fundamental Research Funds for the Central Universities (lzujbky-2016-249 and
728 lzujbky-2016-253). We thank Dr. Vitali Fioletov for his suggestions and advices
729 during the ~~course of~~ preparation of this manuscript.

730

731 **Reference**

732 Assareh, N., Prabamroong, T., Manomaiphiboon, K., Theramongkol, P., Leungsakul,
733 S., Mitritjit, N., and Rachiwong, J.: Analysis of observed surface ozone in the dry
734 season over Eastern Thailand during 1997–2012, *Atmos. Res.*, 178, 17-30, doi:
735 10.1016/j.atmosres.2016.03.009, 2016.

736 Bauduin, S., Clarisse, L., Hadji-Lazaro, J., Theys, N., Clerbaux, C., and Coheur, P. F.:
737 Retrieval of near-surface sulfur dioxide (SO₂) concentrations at a global scale
738 using IASI satellite observations, *Atmos. Meas. Tech.*, 9, 721-740, doi:
739 10.5194/amt-9-721-2016, 2016.

740 BIEE (British Institute of Energy Economics): BP Statistical Review of World
741 Energy June 2016, Available at:

742 <http://www.bp.com/content/dam/bp/pdf/energy-economics/statistical-review-2016>
743 [/bp-statistical-review-of-world-energy-2016-full-report.pdf](#) (last access: 21
744 January 2017), 2016.

745 [Brasseur, G. P., Hauglustaine, D. A., Walters, S., Rasch, P. J., Müller, J. F., Granier,](#)
746 [C., and Tie, X. X.: MOZART, a global chemical transport model for ozone and](#)
747 [related chemical tracers: 1. Model description, J Geophys. Res., 103,](#)
748 [28265–28289, doi: 10.1029/98JD02397, 1998.](#)

749 Chen, J., Cheng, S., Song, M., and Wang, J.: Interregional differences of coal
750 carbon dioxide emissions in China, *Energ. Policy*, 96, 1–13, doi:
751 10.1016/j.enpol.2016.05.015, 2016.

752 CRGECR (The Comprehensive Research Group for Energy Consulting and
753 Research): Strategy on the Development of Energy “Golden Triangle”,
754 *Engineering Science.*, 9, 18-28, 2015 (in Chinese).

755 CSC (China's State Council): China National Environmental Protection Plan in the
756 11th Five-year (2006-2010), Available at:
757 http://www.gov.cn/zwggk/2007-11/26/content_815498.htm (last access: 21 January
758 2017), 2007 (in Chinese).

759 CSC (China's State Council): Circular on accelerating the number of comments on
760 shutting down small thermal power units in China, Available at
761 http://www.gov.cn/zwggk/2007-01/26/content_509911.htm (last access: 21 January
762 2017), 2011a (in Chinese).

763 CSC (China's State Council): China National Environmental Protection Plan in the

764 12th Five-year (2011-2015), Available at:
765 http://www.gov.cn/zwggk/2011-12/20/content_2024895.htm (last access: 21
766 January 2017), 2011b (in Chinese).

767 CSC (China's State Council): Air Pollution Prevention and Control Action Plan,
768 Available at: http://www.gov.cn/zhengce/content/2013-09/13/content_4561.htm
769 (last access: 21 January 2017), 2013a (in Chinese).

770 CSC (China's State Council): Determination, Measures and Strength-Lanzhou
771 pollution control reproduce the blue sky, Available at:
772 http://www.gov.cn/jrzq/2013-02/03/content_2325835.htm (last access: 21 January
773 2017), 2013b (in Chinese).

774 Cui, Y., Lin, J., Song, C., Liu, M., Yan, Y., Xu, Y., and Huang, B.: Rapid growth in
775 nitrogen dioxide pollution over Western China, 2005-2013. *Atmos. Chem. Phys.*,
776 16, 6207-6221, doi: 10.5194/acp-16-6207-2016, 2016.

777 Diao, X., Zhang, Y., and Chen, K. Z.: The global recession and China's stimulus
778 package: A general equilibrium assessment of country level impacts, China. *Econ.*
779 *Rev.*, 23, 1-17, doi: 10.1016/j.chieco.2011.05.005, 2012.

780 Dou, L.: A research on the impact of industrialization on the environment in
781 Xinjiang with an empirical analysis, Mater thesis, Xinjiang University, Urumqi,
782 2009 (in Chinese).

783 Fathian, F., Dehghan, Z., Bazrkar, M. H., and Eslamian, S.: Trends in hydrological
784 and climatic variables affected by four variations of the Mann-Kendall approach
785 in Urmia Lake Basin, Iran. *Hydrolog. Sci. J.*, 61, 892-904, doi:

786 10.1080/02626667.2014.932911, 2016.

787 Fioletov, V. E., McLinden, C. A., Krotkov, N., and Li, C.: Lifetimes and emissions of
788 SO₂ from point sources estimated from OMI, *Geophys. Res. Lett.*, 42, 1969-1976,
789 doi: 10.1002/2015GL063148, 2015.

790 Fioletov, V. E., McLinden, C. A., Krotkov, N., Li, C., Joiner, J., Theys, N., Carn, S.,
791 and Moran, M. D.: A global catalogue of large SO₂ sources and emissions derived
792 from the Ozone Monitoring Instrument, *Atmos. Chem. Phys.*, 16, 11497–11519,
793 doi: 10.5194/acp-16-11497-2016, 2016.

794 Gao, T., and Shi, X.: Spatio-temporal characteristics of extreme precipitation events
795 during 1951-2011 in Shandong, China and possible connection to the large scale
796 atmospheric circulation, *Stoch. Env. Res. Risk. A.*, 30, 1421-1440, doi:
797 10.1007/s00477-015-1149-7, 2016.

798 Han, Y.; Gao, J.; Li, H; and Li, Y.: Ecological suitability analysis on the industry
799 overall arrangement plan of Ningdong energy sources and chemical industry base,
800 *Environ. Sci. Manager*, 32, 142-147,2007 (in Chinese).

801 He, D., Zhang, Z., and Zhang, W.: How large will be the effect of China's fiscal
802 stimulus package on output and employment, *Pacific Economic Review*, 14,
803 730-744, doi: 10.1111/j.1468-0106.2009.00480.x, 2009.

804 Huang, T., Jiang, W., Ling, Z., Zhao, Y., Gao, H., and Ma, J.: Trend of cancer risk of
805 Chinese inhabitants to dioxins due to changes in dietary patterns 1980-2009, *Sci.*
806 *Rep.*, 6, doi: 10.1038/srep21997, 2016.

807 Ialongo, I., Hakkarainen, J., Kivi, R., Anttila, P., Krotkov, N. A., Yang, K., Li, C.,

808 Tukiainen, S., Hassinen, S., and Tamminen, J.: Comparison of operational
809 satellite SO₂ products with ground-based observations in northern Finland during
810 the Icelandic Holuhraun fissure eruption, *Atmos. Meas. Tech.*, 8, 2279-2289, doi:
811 10.5194/amt-8-2279-2015, 2015.

812 Jiang, J., Zha, Y., Gao, J., and Jiang, J.: Monitoring of SO₂ column concentration
813 change over China from Aura OMI data, *Int. J. Remote Sen.*, 33, 1934-1942, doi:
814 10.1080/01431161.2011.603380, 2012.

815 Kanada, M., Dong, L., Fujita, T., Fujita, M., Inoue, T., Hirano, Y., Togawa, T., and
816 Geng, Y.: Regional disparity and cost-effective SO₂ pollution control in China: A
817 case study in 5 mega-cities, *Energ. Policy*, 61, 1322-1331,
818 doi:10.1016/j.enpol.2013.05.105, 2013.

819 Kendall, M. G., and Charles, G.: Rank correlation methods, Oxford Univ. Press,
820 New York., USA, 202 pp., 1975.

821 [Krotkov, N. A., Carn, S. A., Krueger, A. J., Bhartia, P. K., and Yang, K.: Band](#)
822 [Residual Difference Algorithm for Retrieval of SO₂ From the Aura Ozone](#)
823 [Monitoring Instrument \(OMI\), *IEEE T. Geosci. Remote*, 44, 1259-1266,](#)
824 [doi:10.1109/TGRS.2005.861932, 2006.](#)

825 [Krotkov, N. A., McClure, B., Dickerson, R. R., Carn, S. A., Li, C., Bhartia, P. K.,](#)
826 [Yang, K., Krueger, A. J., Li, Z., Levelt, P. F., Chen, H., Wang, P., and Lu, D.:](#)
827 [Validation of SO₂ retrievals from the Ozone Monitoring Instrument over NE](#)
828 [China, *J. Geophys. Res.*, 113, D16S40, doi:10.1029/2007JD008818, 2008.](#)

829 [Krotkov, N. A., McLinden, C. A., Li, C., Lamsal, L. N., Celarier, E. A., Marchenko,](#)

830 S. V., Swartz, W. H., Bucsela, E. J., Joiner, J., Duncan, B. N., Boersma, K. F.,
831 Veefkind, J. P., Levelt, P. F., Fioletov, V. E., Dickerson, R. R., He, H., Lu, Z., and
832 Streets, D. G.: Aura OMI observations of regional SO₂ and NO₂ pollution changes
833 from 2005 to 2015, *Atmos. Chem. Phys.*, 16, 4605-4629, doi:
834 10.5194/acp-16-4605-2016, 2016.

835 Kurokawa, J., Ohara, T., Morikawa, T., Hanayama, S., Greet, J. M., G., Fukui, T.,
836 Kawashima, K., and Akimoto, H.: Emissions of air pollutants and greenhouse
837 gases over Asian regions during 2000–2008: Regional Emission
838 ~~Inventory~~[inventory](#) in Asia (REAS) version 2, *Atmos. Chem. Phys.*, 13,
839 11019–11058, doi: 10.5194/acp-13-11019-2013, 2013.

840 [Levelt, P. F., Van der Oord, G. H. J., Dobber, M. R., Malkki, A., Visser, H., De Vries,](#)
841 [J., Stammes, P., Lundell, J., Saari, H.: The ozone monitoring instrument. *IEEE*](#)
842 [Transactions on Geoscience and Remote Sensing, 44, 1093-1101,](#)
843 [doi:10.1109/TGRS.2006.872333, 2006a.](#)

844 [Levelt, P. F., Hilsenrath, E., Leppelmeier, G. W., Oord, G. H. J. Van Den, Bhartia, P.](#)
845 [K., Tamminen, J., De Haan, J. F., and Veefkind, J. P.: Science Objectives of the](#)
846 [Ozone Monitoring Instrument, *IEEE T. Geosci. Remote Sens.*, 44, 1199-1208,](#)
847 [2006b.](#)

848 Li, C., Joiner, J., Krotkov, N. A., and Bhartia, P. K.: A fast and sensitive new satellite
849 SO₂ retrieval algorithm based on principal component analysis: Application to the
850 Ozone Monitoring Instrument, *Geophys. Res. Lett.*, 40, 6314-6318, doi:
851 10.1002/2013GL058134,2013.

852 Li, C., Wang, R., Ning, H., and Luo, Q.: Changes in climate extremes and their
853 impact on wheat yield in Tianshan Mountains region, northwest China, *Environ.*
854 *Earth Sci.*, 75, doi: 10.1007/s12665-016-6030-6, 2016.

855 Li, C., Zhang, Q., Krotkov, N. A., Streets, D. G., He, K., Tsay, S. C., and Gleason, J.
856 F.: Recent large reduction in sulfur dioxide emissions from Chinese power plants
857 observed by the Ozone Monitoring Instrument, *Geophys. Res. Lett.*, 37, L08807,
858 doi: 10.1029/2010GL042594, 2010.

859 Li, M., Zhang, Q., Kurokawa, J., Woo, J., He, K., Lu, Z., Ohara, T., Song, Y., Streets,
860 D. G., Carmichael, G. R., Cheng, Y., Hong, C., Huo, H., Jiang, X., Kang, S., Liu,
861 F., Su, H., and Zheng, B.: MIX: a mosaic Asian anthropogenic emission inventory
862 under the international collaboration framework of the MICS-Asia and HTAP,
863 *Atmos. Chem. Phys.*, 17, 935-963, doi: 10.5194/acp-17-935-2017, 2017.

864 | Lu, Z., Streets, D. G., Zhang, Q., Wang, S., Carmichael, G. R., Cheng, Y. F., Wei, C.,
865 Chin, M., Diehl, T., and Tan, Q.: Sulfur dioxide emissions in China and sulfur
866 trends in East Asia since 2000, *Atmos. Chem. Phys.*, 10, 6311-6331, doi:
867 10.5194/acp-10-6311-2010, 2010.

868 Lu, Z., Zhang, Q., and Streets, D. G.: Sulfur dioxide and primary carbonaceous
869 aerosol emissions in China and India, 1996-2010, *Atmos. Chem. Phys.*, 11,
870 9839-9864, doi: 10.5194/acp-11-9839-2011, 2011.

871 Ma, J., and Xu, J.: China's energy rush harming ecosystem, *Nature*, 541-30, doi:
872 10.1038/541030b, 2017.

873 Mann, H. B.: Nonparametric tests against trend, *Econometrica*, 13, 245-259, doi:

874 10.2307/1907187, 1945.

875 McLinden, C. A., Fioletov, V., [Boersma, K. F., Kharol, S. K., Krotkov, N., Lamsal,](#)
876 [L., Makar, P. A., Martin, R. V., Veefkind, J. P., and Yang, K.: Improved satellite](#)
877 [retrievals of NO₂ and SO₂ over the Canadian oil sands and comparisons with](#)
878 [surface measurements, Atmos. Chem. Phys., 14, 3637–3656,](#)
879 [doi:10.5194/acp-14-3637-2014, 2014.](#)

880 [McLinden, C. A., Fioletov, V.,](#) Krotkov, N. A., Li, C., Boersma, K. F., and Adams, C.:
881 A decade of change in NO₂ and SO₂ over the Canadian oil sands as seen from
882 space, Environ. Sci. Technol., 50, 331-337, doi: 10.1021/acs.est.5b04985, 2015.

883 McLinden, C. A., Fioletov, V., Shephard, M. W., Krotkov, N., Li, C., Martin, R. V.,
884 Moran, M. D., and Joiner, J.: Space-based detection of missing sulfur dioxide
885 sources of global air pollution, Nature Geosci., 9, 496-500, doi: 10.1038/ngeo2724,
886 2016.

887 MEPC (Ministry of Environmental Protection of China): Ambient air quality
888 standards, Available at:
889 http://kjs.mep.gov.cn/hjbhzbz/bzwb/dqhjbh/dqhjzlbz/201203/t20120302_224165.s
890 [html](#) (last access:21 January 2017), 2012 (in Chinese).

891 Moraes, J. M., Pellegrino, G. Q., Ballester, M. V., Martinelli, L. A., Victoria, R. L.,
892 and Krusche, A. V.: Trends in hydrological parameters of a southern Brazilian
893 watershed and its relation to human induced changes, Water Resour. Manag., 12,
894 295-311, doi: 10.1023/A:1008048212420, 1998.

895 NBSC(National Bureau of Statistics of China): China Energy Statistical Yearbook

896 | 2005, China Statistics Press, Beijing, 2005.

897 NBSC(National Bureau of Statistics of China): China Energy Statistical Yearbook
898 2006, China Statistics Press, Beijing, 2006.

899 NBSC(National Bureau of Statistics of China): China Energy Statistical Yearbook
900 | 2011, China Statistics Press, Beijing, 2011.

901 NBSC(National Bureau of Statistics of China): China Energy Statistical Yearbook
902 | 2015, China Statistics Press, Beijing, 2015.

903 Ohara, T., Akimoto, H., Kurokawa, J., Horii, N., Yamaji, K., Yan, X., and Hayasaka,
904 T.: An Asian emission inventory of anthropogenic emission sources for the period
905 1980–2020, *Atmos. Chem. Phys.*, 7, 4419-4444, doi: 10.5194/acp-7-4419-2007,
906 2007.

907 Sharma, C. S., Panda, S. N., Pradhan, R. P., Singh, A., and Kawamura, A.:
908 Precipitation and temperature changes in eastern India by multiple trend detection
909 methods, *Atmos. Res.*, 180, 211-225, doi: 10.1016/j.atmosres.2016.04.019,
910 2016.

911 Shen, Y., Zhang, X., Brook, J. R., Huang, T., Zhao, Y., Gao, H., and Ma, J.: Satellite
912 remote sensing of air quality in the Energy Golden Triangle in Northwest China,
913 *Environ. Sci. Technol. Lett.*, 3, 275-279, doi: 10.1021/acs.estlett.6b00182, 2016.

914 Sicard, P., Serra, R., and Rossello, P.: Spatiotemporal trends in ground-level ozone
915 concentrations and metrics in France over the time period 1999-2012, *Environ.*
916 *Res.*, 149, 122-144, doi:10.1016/j.envres.2016.05.014, 2016.

917 Smith, S. J., van Aardenne, J., Klimont, Z., Andres, R. J., Volke, A., and Delgado

918 Arias, S.: Anthropogenic sulfur dioxide emissions: 1850-2005, *Atmos. Chem.*
919 *Phys.*, 11, 1101-1116, doi:10.5194/acp-11-1101-2011, 2011.

920 Stevenson, D. S., Johnson, C. E., Collins, W. J., and Derwent, R. G.: The atmospheric
921 sulphur cycle and the role of volcanic SO₂, *Geol. Soc. Lond. Spec. Publ.*, 213,
922 295-305, doi: 10.1144/GSL.SP.2003.213.01.18, 2003.

923 Su, S., Li, B., Cui, S., and Tao, S.: Sulfur Dioxide Emissions from Combustion in
924 China: From 1990 to 2007, *Environ. Sci. Technol.*, 45, 8403-8410, doi:
925 10.1021/es201656f, 2011.

926 Waked, A., Sauvage, S., Borbon, A., Gauduin, J., Pallares, C., Vagnet, M. P., Thierry,
927 L., and Locoge, N.: Multi-year levels and trends of non-methane hydrocarbon
928 concentrations observed in ambient air in France, *Atmos. Environ.*, 141, 263-275,
929 doi: 10.1016/j.atmosenv.2016.06.059, 2016.

930 Wang, S., Zhang, Q., Martin, R.V., Philip, S., Liu, F., Li, M., Jiang, X., and He, K.:
931 Satellite measurements oversee China's sulfur dioxide emission reductions from
932 coal-fired power plants, *Environ. Res. Lett.*, 10, 114015, doi:
933 10.1088/1748-9326/10/11/114015, 2015.

934 Wang, S., Satellite remote sensing of the sulfur dioxide and nitrogen dioxide
935 emissions from coal-fired power plants, PhD thesis, Tsinghua University, Beijing,
936 2014.

937 Wang, Z., Shao, M., Chen, L., Tao, M., Zhong, L., Chen, D., Fan, M., Wang, Y., and
938 Wang, X.: Space view of the decadal variation for typical air pollutants in the
939 Pearl River Delta (PRD) region in China, *Front. Env. Sci. Eng.*, 10, doi:

940 10.1007/s11783-016-0853-y, 2016.

941 Whelpdale, D. M., Dorling, S. R., Hicks, B. B., and Summers, P.W.: Atmospheric
942 process in: Global Acid Deposition Assessment, edited by: Whelpdale, D. M., and
943 Kaiser, M. S., World Meteorological Organization Global Atmosphere Watch,
944 Report Number 106, Geneva, 7-32, 1996.

945 Yan, H., Chen, L., Su, L., Tao, J., and Yu, C.: SO₂ columns over China: Temporal
946 and spatial variations using OMI and GOME-2 observations, 35th International
947 Symposium on Remote Sensing of Environment, 17, 012027, doi:
948 10.1088/1755-1315/17/1/012027, 2014.

949 Yue, S and Pilon, P.: A comparison of the power of the t-test, Mann-Kendall and
950 bootstrap tests for trend detection, Hydrolog. Sci. J., 49, 21-37, doi:
951 10.1623/hysj.49.1.21.53996, 2004.

952 Yue, S., and Wang, C.: The Mann-Kendall test modified by effective sample size to
953 detect trend in serially correlated hydrological series, Water Resour. Manag., 18,
954 201-218, doi: 10.1023/B:WARM.0000043140.61082.60, 2004.

955 Zhang, X., Huang, T., Zhang, L., Gao, H., Shen, Y., and Ma, J.: Trends of deposition
956 fluxes and loadings of sulfur dioxide and nitrogen oxides in the artificial Three
957 Northern Regions Shelter Forest across northern China, Environ. Pollut., 207, doi:
958 10.1016/j.envpol.2015.09.022 238-247, 2015.

959 Zhang, X., Huang, T. Zhang, L., Shen, Y., Zhao, Y., Gao, H., Mao, X., Jia, C., and
960 Ma, J.: Three-North Shelter Forest Program contribution to long-term increasing
961 trends of biogenic isoprene emissions in northern China, Atmos. Chem. Phys., 16,

962 6949-6960, doi: 10.5194/acp-16-6949-2016, 2016.

963 Zhang, Y., Guan, D., Jin, C., Wang, A., Wu, J., and Yuan, F.: Analysis of impacts of
964 climate variability and human activity on stream flow for a river basin in
965 northeast China, *J. Hydrol.*, 410, 239-247, doi: 10.1016/j.jhydrol.2011.09.023,
966 2011.

967 Zhao, B., Wang, S. X., Liu, H., Xu, J. Y., Fu, K., Klimont, Z., Hao, J. M., He, K. B.,
968 Cofala, J., and Amann, M.: NO_x emissions in China: historical trends and future
969 perspectives, *Atmos. Chem. Phys.*, 13, 9869–9897, doi:
970 10.5194/acp-13-9869-2013, 2013.

971 Zhao, [H., Li, X., Zhang, Q., Jiang, X., Lin, J., Peters, G. G., Li, M., Geng, G., Zheng,](#)
972 [B., Huo, H., Zhang, L., Davis, S. J., and He, K.: Effects of atmospheric transport](#)
973 [and trade on air pollution mortality in China, *Atmos. Chem. Phys. Discuss.*,](#)
974 [doi:10.5194/acp-2017-263, in review, 2017.](#)

975 [Zhao, L.:](#) Strategic thinking on construction of Ningdong Energy Chemical Base and
976 development of Ningxia Coal Industry Group, *Northwest Coal*, 4, 11-13, 2016 (in
977 Chinese).

978 Zhao, Y., Huang, T., Wang, L., Gao, H., and Ma, J.: Step changes in persistent
979 organic pollutants over the Arctic and their implications, *Atmos. Chem. Phys.*, 15,
980 3479-3495, doi: 10.5194/acp-15-3479-2015, 2015.

981 Zhao, Y., Nielsen, C. P., Lei, Y., McElroy, M. B., and Hao, J.: Quantifying the
982 uncertainties of a bottom-up emission inventory of anthropogenic atmospheric
983 pollutants in China, *Atmos. Chem. Phys.*, 11, 2295–2308, doi:

984 10.5194/acp-11-2295-2011, 2011.

985 Zhu, J.; and Ruth, M.: Relocation or reallocation: Impacts of differentiated energy
986 saving regulation on manufacturing industries in China, *Ecol. Econ.*, 110,
987 119–133, doi: 10.1016/j.ecolecon.2014.12.020, 2015.

988
989
990

Formatted

Formatted: Space After: 0.5 line, Line spacing: single, Adjust space between Latin and Asian text, Adjust space between Asian text and numbers

991 **Table 1** Annual growth rate for OMI SO₂ VCD and economic activities for
992 individual provinces and municipality during 2005-2014 (%_{yr⁻¹}), and SO₂ emission
993 reduction plan during the 11th and 12th Five-Year Plan period (%).

Region	OMI SO ₂ VCD	coal consumption	Industrial GDP	Thermal power generation	steel production	SO ₂ emission reduction plan (%)		
						2006-2010 ^a	2011-2015 ^b	
Northwest ern	Inner Mongolia	0.94	11.29	20.48	14.07	8.38	-3.8	-3.8
	Shaanxi	-3.41	13.14	19.96	13.01	14.48	-12	-7.9
	Gansu	-0.09	6.69	14.19	8.89	9.92	0	2.0
	Qinghai	0.69	11.20	18.70	9.88	12.37	0	16.7
	Ningxia	0.95	11.79	17.44	15.04	152.71	-9.3	-3.6
	Xinjiang	1.57	17.21	14.21	23.39	16.27	0	0
BTH	Beijing	-3.59	-6.13	9.13	5.99	-48.52	-20.4	-13.4
	Tianjin	-4.63	3.15	15.84	6.01	10.19	-9.4	-9.4
	Hebei	-5.05	4.16	12.37	6.22	10.70	-15	-12.7
YRD	Shanghai	-7.65	-0.93	6.64	0.86	-0.92	-26.9	-13.7
	Jiangsu	-5.93	5.39	12.51	7.49	13.35	-18.0	-14.8
	Zhejiang	-2.07	4.04	11.40	8.68	13.94	-15.0	-13.3
PRD	Guangdong	-4.55	6.15	12.03	5.92	6.87	-15.0	-14.8

994 a and b represents proposed reduction in SO₂ emission in 2010 relative to 2005, and 2015 relative
995 to 2010, respectively. The value for PRD refers to the proposed target for Guangdong Province.

996
997
998
999
1000
1001
1002

Formatted

Formatted: Line spacing: single

1003
1004
1005
1006
1007
1008
1009
1010
1011
1012
1013
1014
1015

Figure Captions

1016

1017

1018

1019

1020

1021

1022

1023

1024

1025

1026

1027

1028

1029

1030

1031

Figure 1 Provinces, autonomous regions, and selected regions in China in this investigation. Northwestern China, defined by pink slash, includes Inner Mongolia, Shaanxi, Gansu, Qinghai, Ningxia, and Xinjiang province. Light green shadings with cross highlight Beijing-Tianjin-Hebei (BTH) and the light green color stands for the North China Plain (NCP, including BTH), ~~defined by light green color,~~ including BTH, Shandong, and Henan province. The Sichuan Basin, Yangtze River Delta (YRD), and Pearl River Delta (PRD) is defined by yellow, pink, and blue color. The Urumqi-Midong region including Midong energy industrial base (MEIB) is defined by brick red. The Energy Golden Triangle (EGT), defined by purple color, including Ningdong energy chemical industrial base (NECIB) in Ningxia, Yulin in Shaanxi, and Erdos in Inner Mongonia. Red triangles indicate 188 monitoring sites across China. Blue solid circles indicate 6 selected cities in Fig. 2. Red triangle indicate 188 monitoring sites across China.—

1032

1033

1034

1035

1036

Figure 2 Annually averaged SO₂ VCD (DU), scaled on the right-hand-side ~~y-axis~~ and measured annual SO₂ air concentration (μg/m³), scaled on the left-hand-side ~~y-axis~~, in Beijing, Shanghai, Chongqing, Guangzhou, Yinchuan, and Urumqi.

1037

1038

1039

1040

Figure 3 Annually averaged SO₂ VCD (DU), scaled on the right-hand-side ~~y-axis~~ and annual emissions (thousand ton/yr) of SO₂ on the left-hand-side ~~y-axis~~ in the NCP, YRD, PRD, Sichuan Basin, EGT, and Urumqi-Midong.

1041

1042

1043

1044

1045

1046

Figure 4 Annual averaging OMI-retrieved vertical column densities of SO₂ (DU) and their trends from 2005 to 2015 on 0.25° × 0.25° latitude/longitude resolution in China. (a). Annual mean SO₂ vertical column densities; (b). slope (trend) of linear regression relationship between annual average OMI-retrieved SO₂ VCD and the time sequence from 2005 to 2015 over China. The positive values indicate an increasing trend of SO₂ VCD from 2005 to 2015, and vice versa. The blue circle

Formatted: Subscript

Formatted: Subscript

1047 highlights the six selected regions where SO₂ VCD displayed dramatic change for
1048 further assessment of the long term trends and step change points in SO₂ VCD.
1049 These six regions are NCP (a), YRD (b), PRD (c), Sichuan Basin (d), Energy Golden
1050 Triangle (EGT, e), and Urumqi-Midong region (f).

1051
1052 **Figure 5** Percentage changes in annual mean OMI SO₂ VCD in the four highlighted
1053 regions in eastern and southern China and two large-scale energy industry
1054 basesparks in the EGT and Urumqi-Midong region in **Figure 4b** (relative to 2005).

1055
1056 ~~**Figure 6** Annual fractions of OMI retrieved SO₂ VCD and emissions~~
1057 ~~averaged over 6 northwestern provinces in the national total SO₂ VCD from 2005 to~~
1058 ~~2015 and emission from 2005 to 2014. (a) fraction of annual mean SO₂ VCD; (b)~~
1059 ~~fraction of annual mean emission. Fractions of SO₂ VCD are calculated as the ratio~~
1060 ~~of the sum of annually averaged SO₂ VCD in northwestern China to the sum of~~
1061 ~~annually averaged SO₂ VCD in the national total from 2005 to 2015 (%).~~

1062 ~~**Figure 7** Per capita SO₂ emission in six provinces of northwestern China and three~~
1063 ~~key eastern regions (tons/person). The value for PRD refers to the per capita SO₂~~
1064 ~~emission for Guangdong province.~~

1065 **Figure 8** Mann-Kendall (MK) test statistics for annually SO₂ VCD in those
1066 highlighted regions (**Figs. 1** and **4b**) from 2005-2015. The blue solid line is the
1067 forward sequence UF_k and the red solid line is the backward sequence UB_k defined
1068 by Eq (5). The positive values for UF_k indicate an increasing trend of SO₂ VCD, and
1069 vice versa. Two straight solid lines stand for confidence interval between -1.96
1070 (straight green line) and 1.96 (straight purple line) in the MK test. The bold black
1071 line in the middle highlights zero value of UF_k and UB_k . The bold black line in the
1072 middle highlights zero value of UF_k and UB_k . The intersection of UF_k and UB_k
1073 sequences within the intervals between two confidence levels indicates a step change
1074 point.

1075
1076 ~~**Figure 7** Annual fractions of OMI retrieved SO₂ VCD and emissions averaged over~~
1077 ~~6 northwestern provinces in the national total SO₂ VCD from 2005 to 2015 and~~
1078 ~~emission from 2005 to 2014. (a) fraction of annual mean SO₂ VCD; (b) fraction of~~
1079 ~~annual mean emission. Fractions of SO₂ VCD are calculated as the ratio of the sum~~
1080 ~~of annually averaged SO₂ VCD in northwestern China to the sum of annually~~
1081 ~~averaged SO₂ VCD in the national total from 2005 to 2015 (%).~~

1082
1083 ~~**Figure 8** Per capita SO₂ emission in six provinces of northwestern China and three~~
1084 ~~key eastern regions (tons/person). The value for PRD refers to the per capita SO₂~~
1085 ~~emission for Guangdong province.~~

1086
1087 **Figure 9** Mann-Kendall (MK) test statistics for annually averaged SO₂ VCD in six
1088 provinces in northwestern China from 2005-2015. The blue solid line is the forward
1089 sequence UF_k and the red solid line is the backward sequence UB_k defined by Eq (5).
1090 The positive values ~~offor~~ UF_k indicate an increasing trend of SO₂ VCD, and vice

1091 versa. Two straight solid lines stand for confidence interval between -1.96 (straight
1092 green line) and 1.96 (straight purple line) in the MK test. The intersection of UF_k and
1093 UB_k sequences within intervals between two confidence levels indicates a step
1094 change point.

1095
1096 **Figure 10** Annually averaging OMI-retrieved vertical column densities of Mean SO₂
1097 (DU)burden estimated by the OMI measured SO₂ VCD (DU) using a new emission
1098 detection algorithm (Fioletov et al., 2016). (a) SO₂ burden in two major point
1099 sources, the MEIB innorthern Xinjiang (a), and the NECIB; (b) SO₂ burden in
1100 Ningxia (b).

Formatted: Adjust space between Latin and Asian text, Adjust space between Asian text and numbers

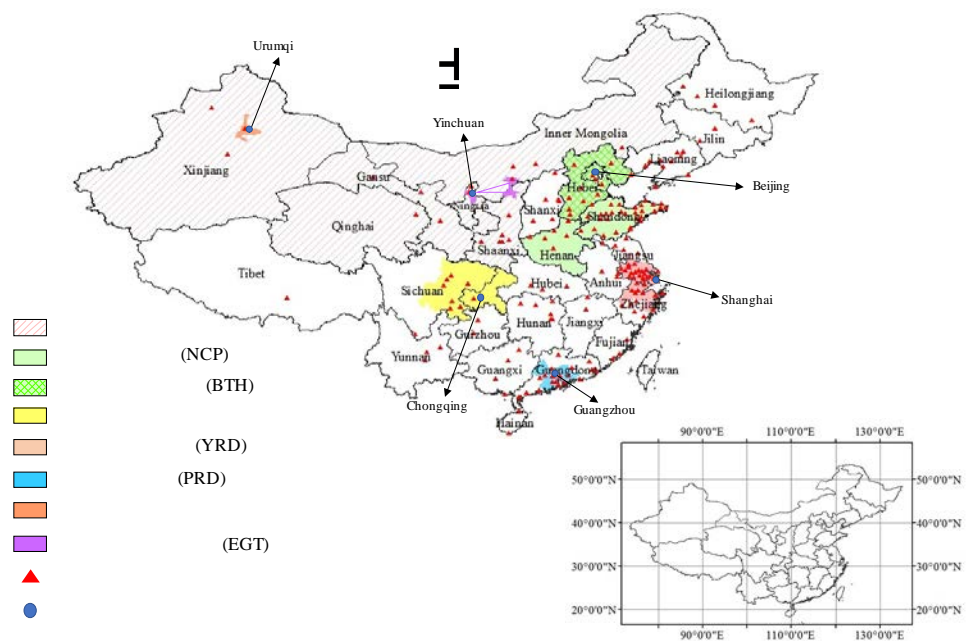
Formatted: Font:

Formatted: Font:

1101
1102 **Figure 11** Annually averaged SO₂ emissions (kt yr⁻¹) and SO₂ VCD (DU)burdens
1103 (10²⁶ molecule) in the NECIB and MEIB, Ningdong and Midong energy industrial
1104 parks and their fractions in provincial total SO₂ emission and ratios between SO₂
1105 VCD in these two regions and that in province. (a). SO₂ emissionburden. (a). SO₂
1106 burden (blue bar) in the NECIBNingdong and its fraction (red solid line) in the total
1107 provincial SO₂ burden in Ningxia; (b). SO₂ burden (blue bar) in Midong and its
1108 fraction (red solid line) in the total provincial SO₂ emission in Ningxia; (b). SO₂
1109 emission (blue bar) in the MEIB and its fraction (red solid line) in the total
1110 provincial SO₂ emissionburden in Xinjiang. (c). SO₂ VCD (blue bar) in the NECIB
1111 and the ratio (red solid line) between SO₂ VCD in the NECIB and that in Ningxia;
1112 (d). SO₂ VCD (blue bar) in the MEIB and the ratio (red solid line) between SO₂
1113 VCD in the MEIB and that in Xinjiang; The left y-axisY-axis stands for SO₂
1114 emission burden and the right y-axisY-axis denotes the fraction (%) at the upper
1115 panel. The left y-axis stands for SO₂ VCD (DU) and the right y-axis denotes the ratio
1116 at the lower panel. The error bars denotes the standard deviations of Source
1117 Detection Algorithm estimated SO₂ emission in two major point sources .

1118
1119
1120
1121
1122

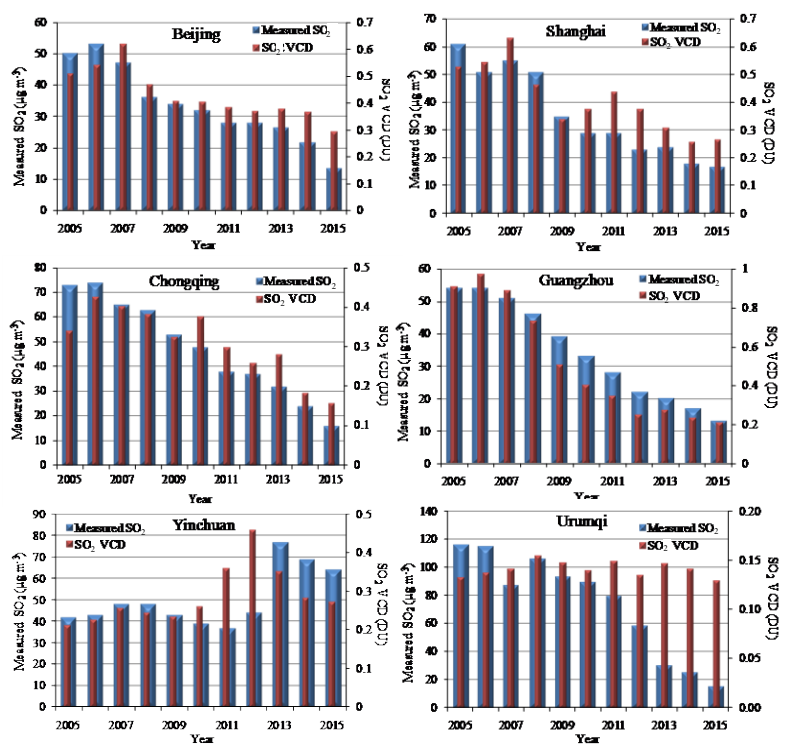
Figure 1



1123
 1124
 1125
 1126
 1127
 1128
 1129
 1130
 1131
 1132
 1133
 1134
 1135
 1136
 1137
 1138
 1139
 1140
 1141
 1142
 1143
 1144
 1145
 1146
 1147
 1148

Figure 2

1149



1150

1151

1152

1153

1154

1155

1156

1157

1158

1159

1160

1161

1162

1163

1164

1165

1166

1167

1168

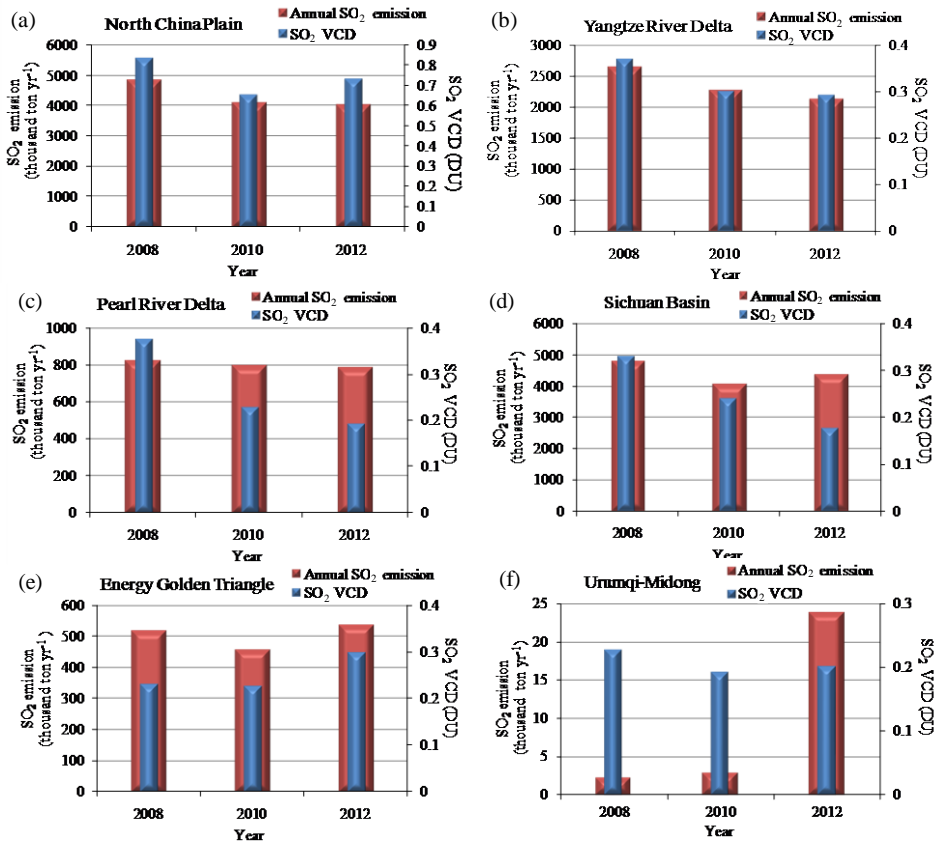
1169

1170

1171

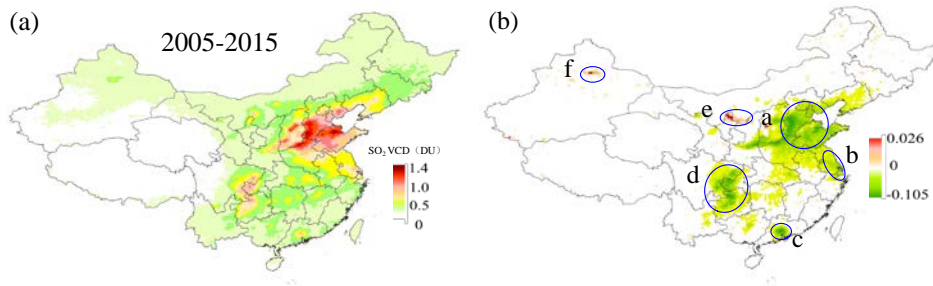
1172

Figure 34

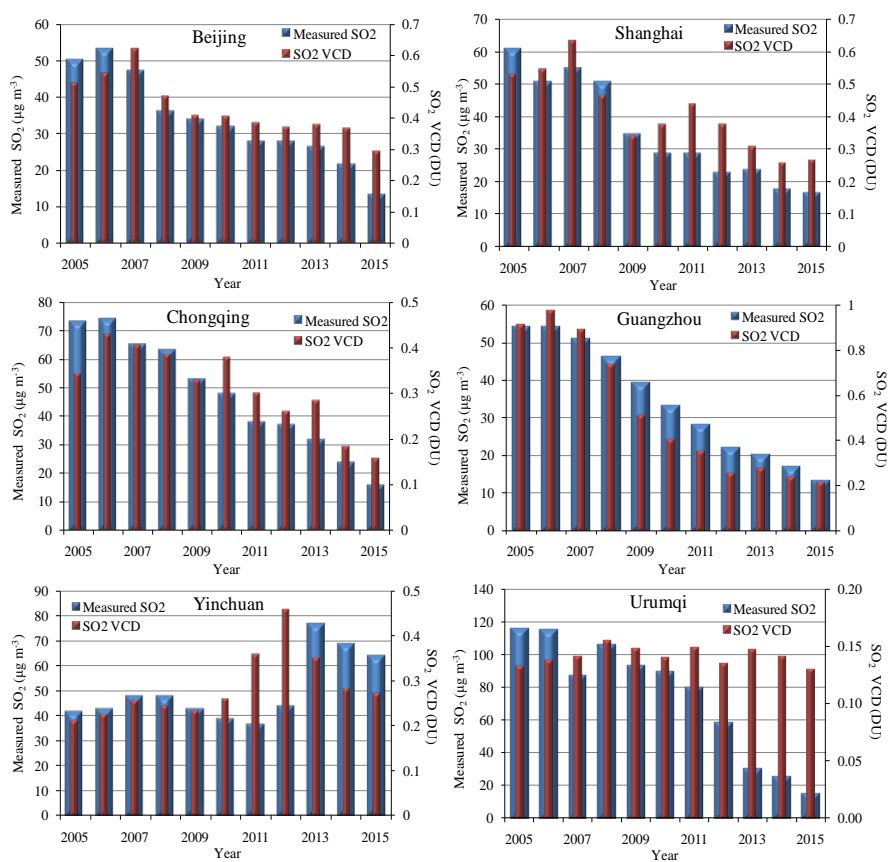


1181
1182
1183
1184
1185
1186
1187
1188
1189
1190
1191
1192
1193
1194
1195
1196
1197
1198
1199
1200
1201
1202
1203
1204
1205

Figure 42

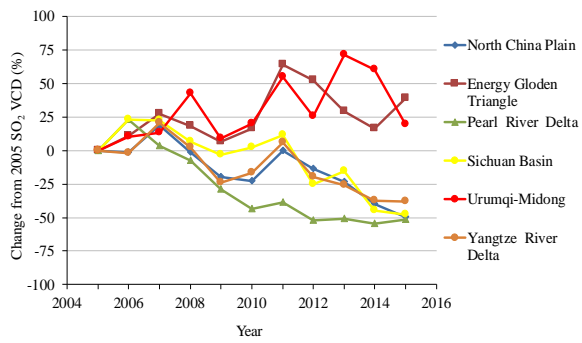


1206

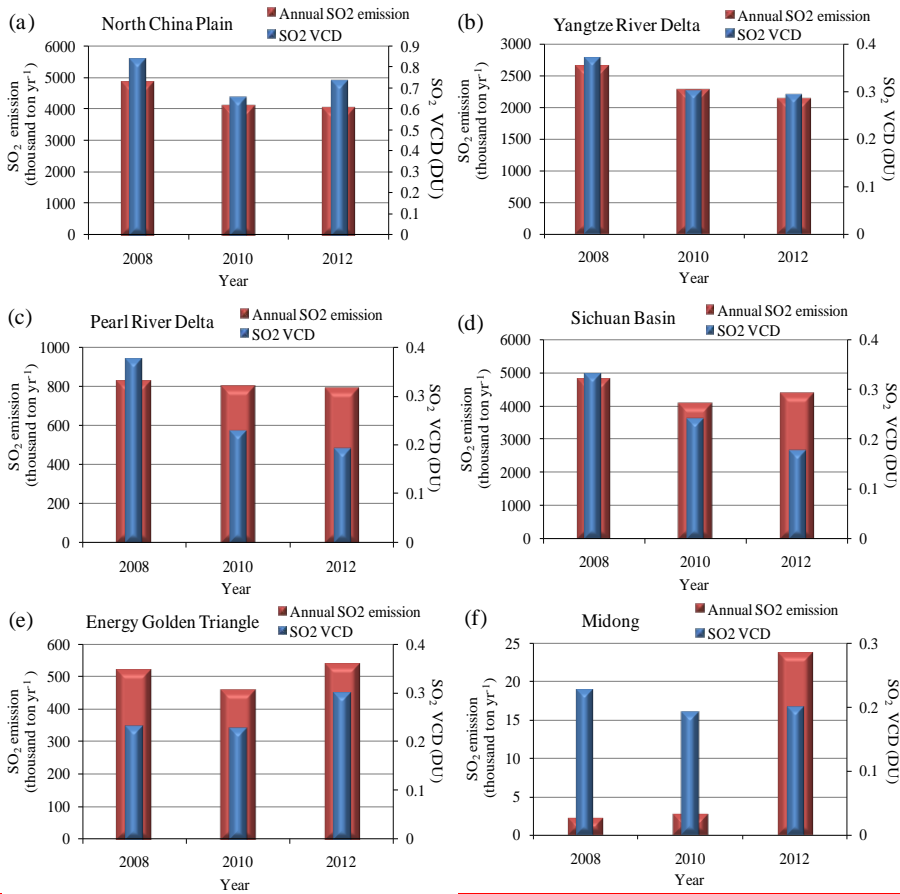


1207
 1208
 1209
 1210
 1211
 1212
 1213
 1214
 1215
 1216
 1217
 1218
 1219
 1220
 1221
 1222
 1223
 1224
 1225
 1226

Figure 53



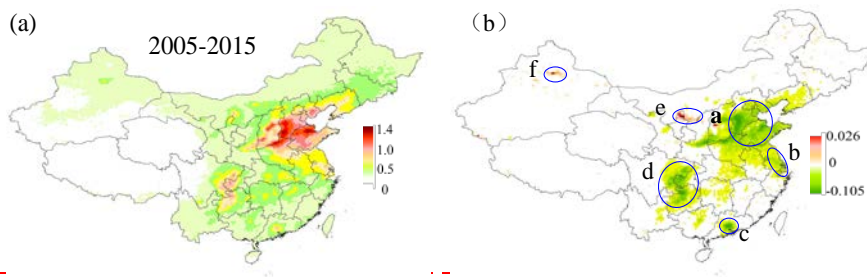
1227
1228
1229
1230
1231



1232
1233
1234
1235
1236

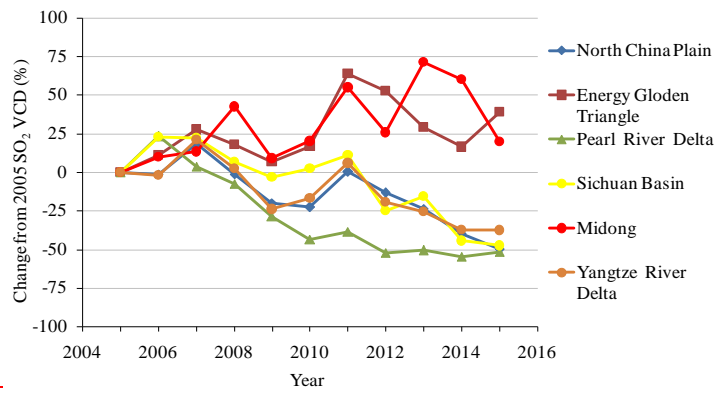
1237
1238
1239
1240
1241
1242
1243
1244
1245
1246
1247
1248
1249
1250

Figure 4



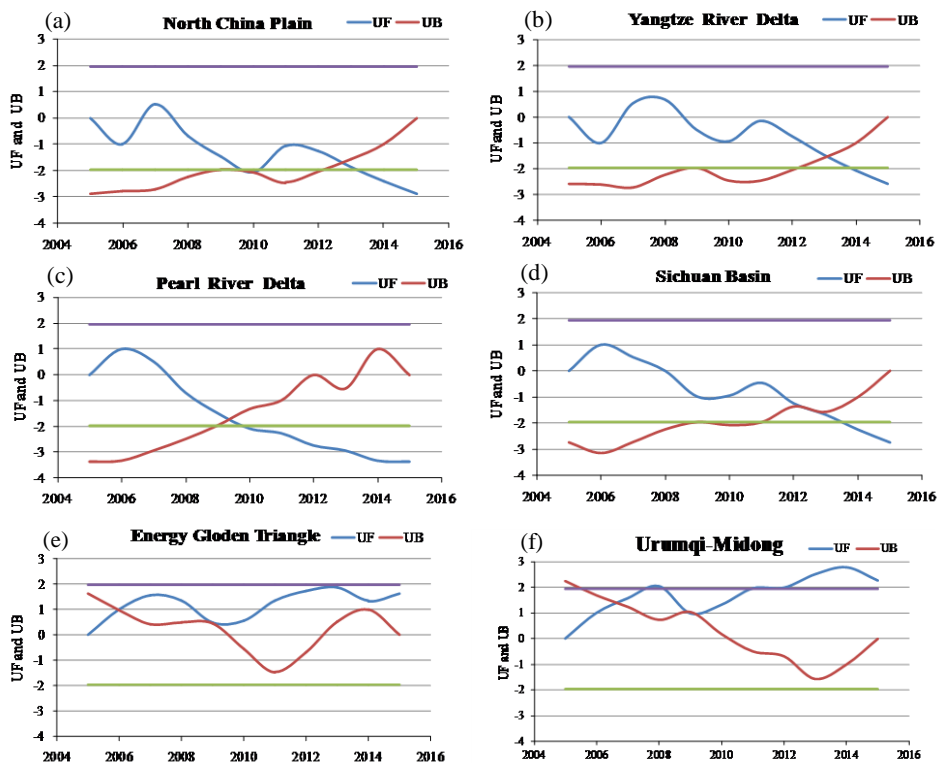
1251
1252
1253
1254
1255
1256
1257
1258
1259
1260
1261
1262
1263

Figure 5

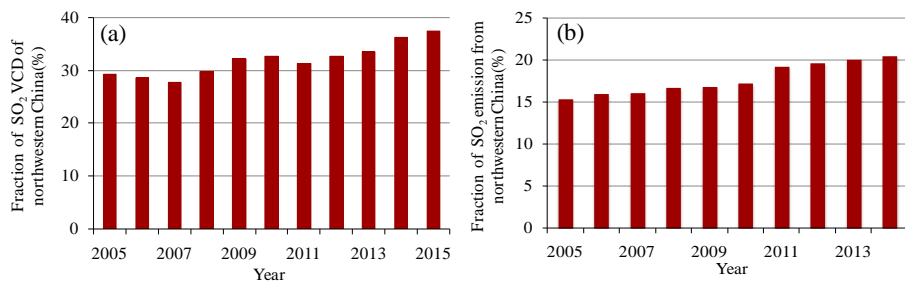


1264
 1265
 1266
 1267
 1268
 1269
 1270
 1271
 1272
 1273
 1274
 1275
 1276

Figure 6



1277



1278

1279

1280

1281

1282

1283

1284

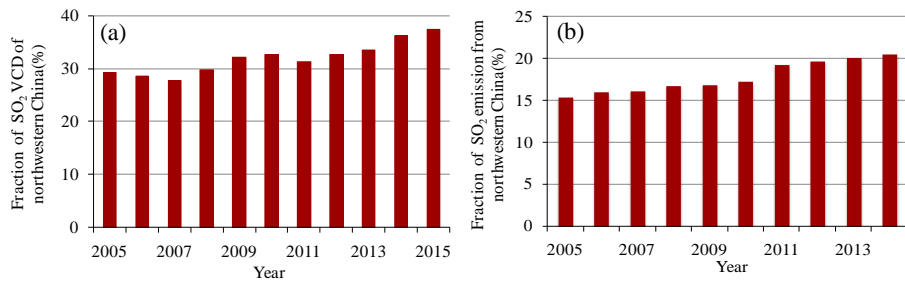
1285

1286

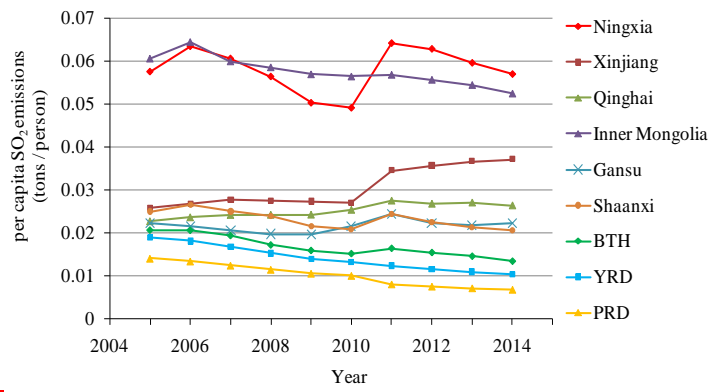
1287

1288 Figure 7

1289



1290



1291

1292

1293

1294

1295

1296

1297

1298

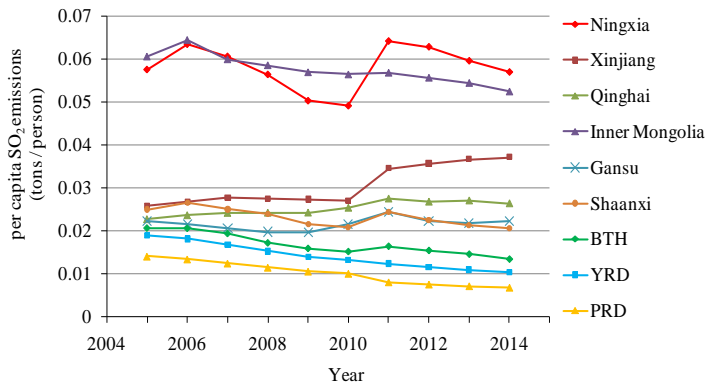
1299

1300

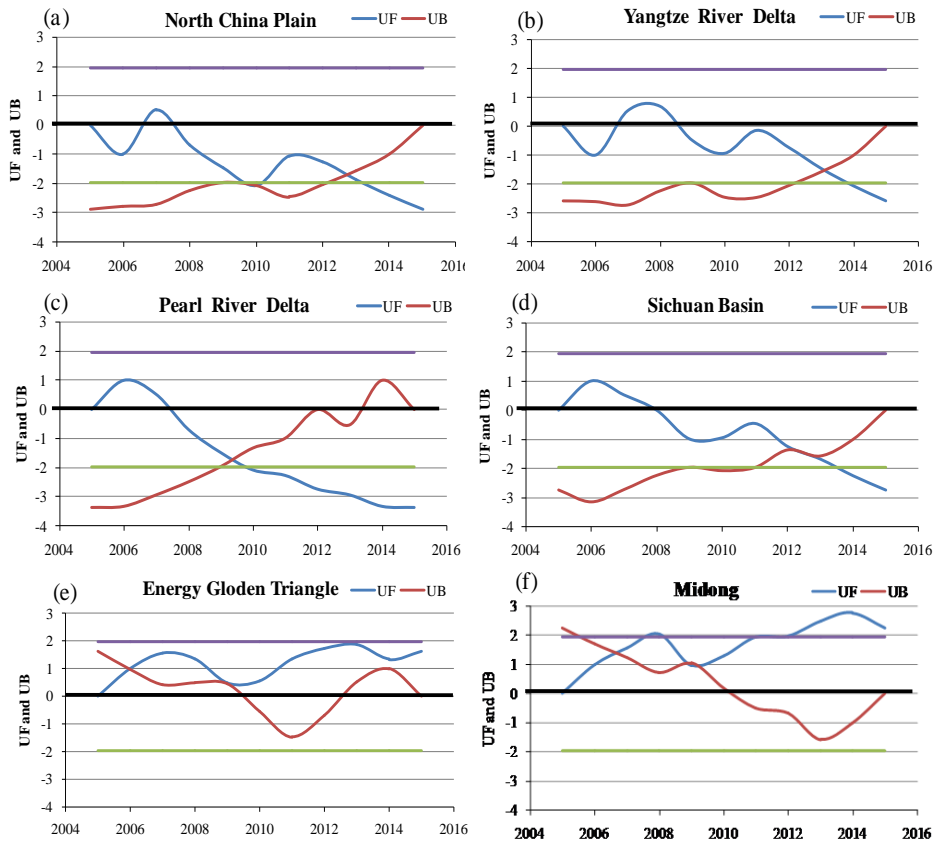
1301

1302 Figure 8

1303



1304



1305

1306

1307

1308

1309

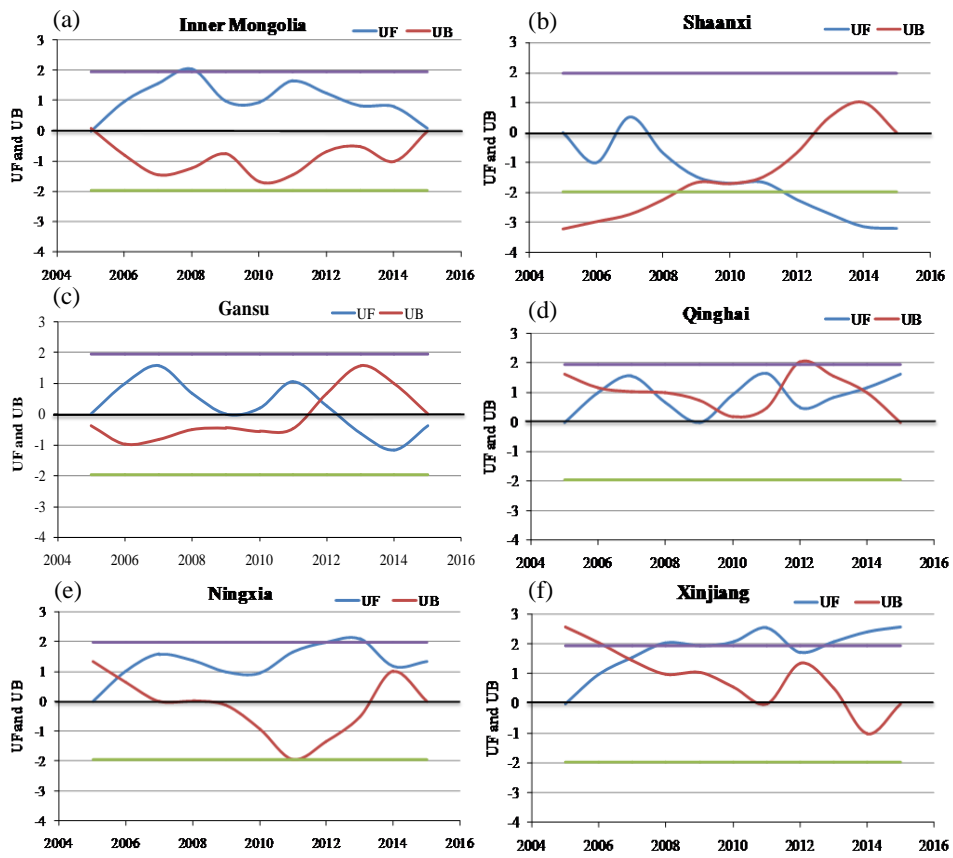
1310

1311

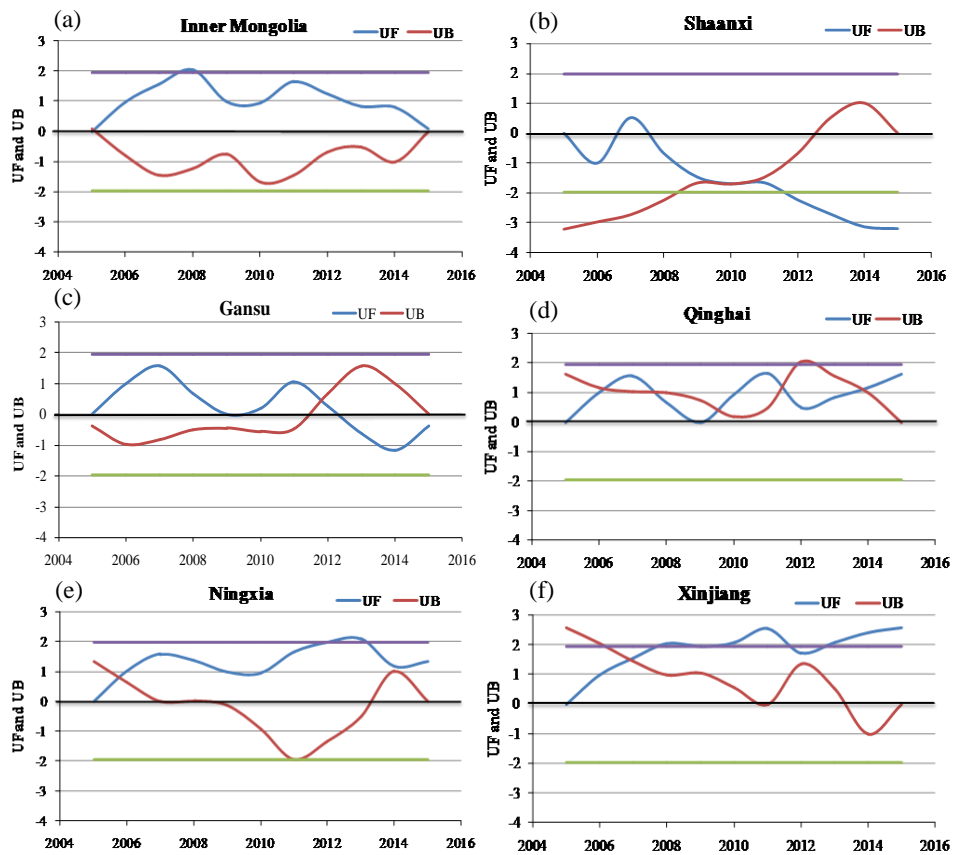
1312

1313
1314
1315
1316
1317
1318
1319
1320
1321
1322
1323
1324

Figure 9



1325



1326

1327

1328

1329

1330

1331

1332

1333

1334

1335

1336

1337

1338

1339

1340

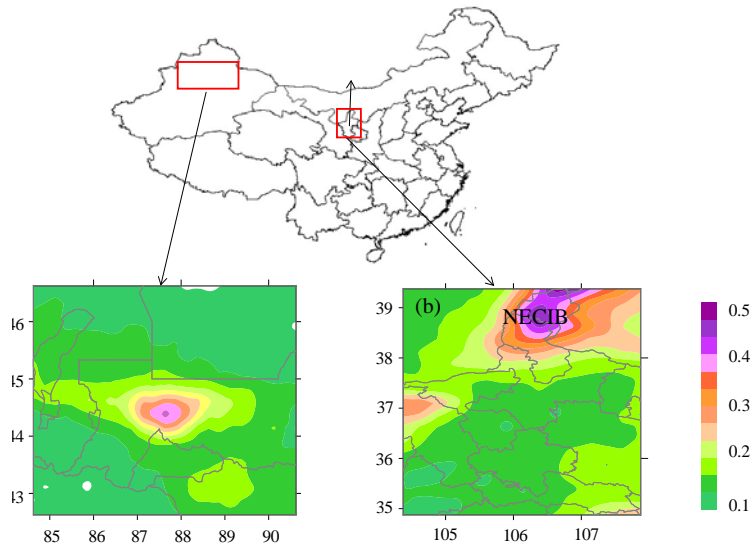
1341

1342

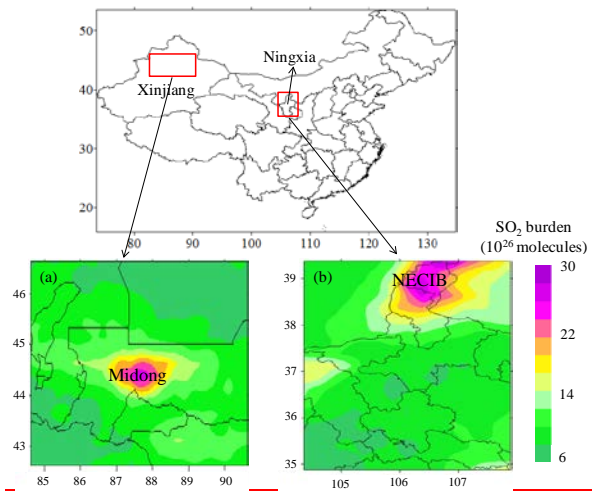
1343

1344 Figure 10

1345



1346



1347

1348

1349

1350

1351

1352

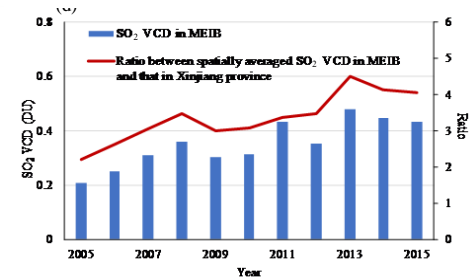
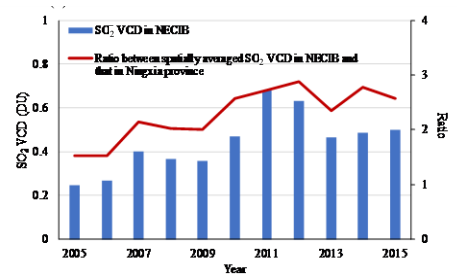
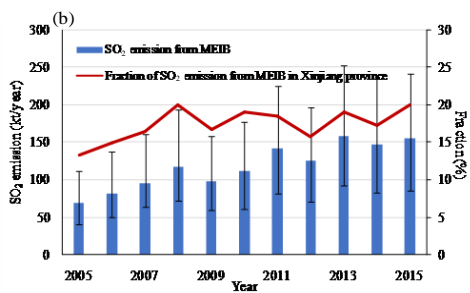
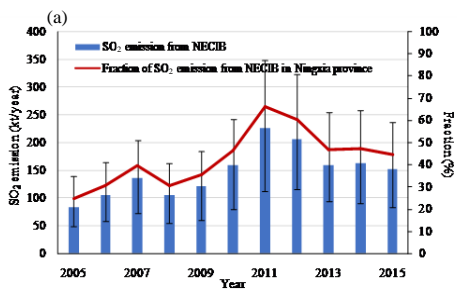
1353

1354

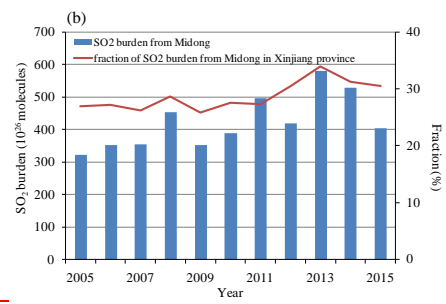
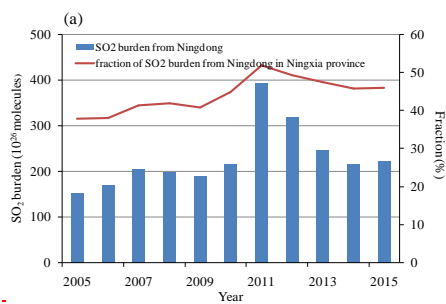
1355

1356

Figure 11



1357



1358

Formatted: Font color: Text 1